Available online at www.sciencedirect.com

ScienceDirect

Solid Earth Sciences 10 (2025) 100231

www.elsevier.com/locate/SESCI

Crystallisation and petrogenesis of Cenozoic alkaline basaltic lavas on the Kapsiki Plateau (Moukoulvi, Far-North Cameroon): Unveiling the mantle's heterogeneity and HIMU signature

Diddi Hamadjoda Djamilatou [a,b,*], Merlin Gountié Dedzo [c], Nils Lenhardt [b], Désiré Tsozué [a], Elvis Asaah Asobo Nkengmatia [d,e], Moussa Klamadji Ngarena [f]

[a] *Department of Earth Sciences, University of Maroua, P.O. Box 814, Maroua, Cameroon*
[b] *Department of Geology, University of Pretoria, Private Bag X20, 0028 Pretoria, South Africa*
[c] *Department of Life and Earth Sciences, High Teachers' Training College, University of Maroua, PO Box 55, Maroua, Cameroon*
[d] *Department of Mines, Ministry of Mines, Industry and Technological Development, P.O. Box 70, Yaounde, Cameroon*
[e] *Department of Earth and Planetary Sciences, Tokyo Institute of Technology, Japan*
[f] *Département des Sciences de la Vie et de la Terre, Faculté des Sciences Techniques et de la Technologie, University of Pala, Pala, Chad*

Received 10 May 2024; revised 27 February 2025; accepted 28 February 2025
Available online 3 April 2025

Abstract

The Kapsiki Plateau represents the northernmost extension of the Cameroon Volcanic Line (CVL) in West Africa. Unlike other regions of the CVL, this area is characterised by a higher prevalence of felsic and intermediate rocks compared to basaltic ones. Detailed investigations into the petrogenetic evolution of these rocks are currently limited. For this reason, Cenozoic alkaline basaltic lavas from the Kapsiki Plateau (Moukoulvi) were studied to enhance comprehension of their crystallisation process, genetic evolution of the magma, and insights into its petrogenesis and source mineralogy. The examined lavas are comparable to the mafic lavas that span the whole range of the CVL and demonstrate major and trace element characteristics similar to those seen in ocean island basalts (OIB). The major and trace element compositions suggest fractional crystallisation mainly including olivine, clinopyroxene, and Fe–Ti oxide with evidence of crustal contamination. The multi-element diagrams reveal consistency with those reported from other CVL volcanoes, displaying depletion of heavy rare earth elements (HREE) and enrichment of light rare elements (LREE), indicating an enriched source and the existence of garnet. The studied lavas have high large ion lithophile element (LILE) contents (Sr = 812–1065 ppm, Ba = 394–467 ppm) relative to high field strength elements (HFSE) (Sr/Zr = 3.97–4.94; average OIB = ~1 Ba/La = 9.42–11.72; average OIB = 9.4). They also have Zr/Sm ratios (26.93–29.88) that are similar to the average OIB (Zr/Sm = 28). Moreover, the studied lavas exhibit elevated levels of incompatible trace elements (e.g., Rb, Pr, U, and Th), as well as higher Ta/Yb and Th/Yb ratios compared to normal OIB values, associated with a notable fluctuation in Nb/Ta and Zr/Hf ratios. The correlations between Th, La, U, and SiO_2, coupled with the trend of the samples on Nb/Y *vs.* Rb/Y diagrams, indicate the influence of crustal contamination on the lavas' composition. The source of these lavas was a heterogeneous source with less than 4 % garnet that underwent partial melting of less than 2 %. The presence of a Pb depletion (Ce/Pb > 30) also implies that these magmas belong to the high μ (HIMU)-OIB type, attributed to lithospheric mantle metasomatism. The formation of these magmas involved partial melting of a mantle source evolving chemically and mineralogically over time with a HIMU composition at very low temperatures. Hydrous minerals, such as phlogopite or amphibole, may indicate modal metasomatism, supported by high Rb/Sr ratios or K_2O high levels. Sr/Zr ratios (3.97–4.94) above OIB values (0.8–1.5) suggest Sr and Ba-rich fluid influence. Elevated Zr/Sm ratios (>28) and variations in Nb/Ta and Zr/Hf ratios point to metasomatic fluids or melts altering the mantle's composition. Therefore, the Moukoulvi lavas, like many CVL alkaline lavas, likely erupted from a metasomatized mantle source that was enriched in incompatible trace elements (Rb, Ba, Ce, Nb, and Zr). This enrichment is reflected in the elevated concentrations of these incompatible trace elements, as well as the relative enrichment in HFSE. The absence of temperature anomalies in the upper mantle beneath the CVL suggests that the magmatism originates from the lithospheric mantle source rather than a mantle plume.

* Corresponding author. Department of Earth Sciences, University of Maroua, P.O. Box 814, Maroua, Cameroon.
E-mail address: diddidjamilatou690@gmail.com (D.H. Djamilatou).

https://doi.org/10.1016/j.sesci.2025.100231

Keywords: Cameroon Volcanic Line; Kapsiki Plateau; Fractional crystallisation; Petrogenesis; Metasomatism; Sub-continental lithospheric mantle

1. Introduction

Volcanological research in Africa is notoriously underdeveloped, and apart from the major active stratovolcanoes along the East African Rift System (Rolet et al., 1991; Wheeler and Karson 1994; Barrat et al., 2000; Zeigler and Cloetingh 2004; Chorowicz 2005; Furman et al., 2007; Biggs et al., 2011; Hutchison et al., 2016; Rooney et al., 2020; Albino and Biggs 2021) or the CVL (Suh et al., 2003; Lapi et al., 2006; Yokoma et al., 2007; Njome et al., 2008; Tsafack et al., 2009; Tchouankoue et al., 2012; Njome and de Wit 2014; Asaah et al., 2015a, 2015b, 2020, 2021; Geiger et al., 2016; Okomo Atouba et al., 2016; Yamgouot et al., 2016, 2018; Ziem à Bidias et al., 2018; Ngwa et al., 2019; Gountié Dedzo et al., 2019, 2020, 2022; Sababa et al., 2021; Njombie Wagsong et al., 2021), the larger part of these volcanic areas that have been active since the Paleogene remains largely unknown to this day. One of these areas is the northernmost segment of the CVL, which has received little attention due to its remoteness and insecure political situation. However, this area holds the potential to provide important new information about how the northern part of the CVL has developed.

The CVL, a series of alkaline volcanoes that have been active from the Paleogene to the present, is a significant magmato-tectonic province on the African plate (Fitton, 1987; Déruelle et al., 2007; Nkouathio et al., 2008; Njonfang et al., 2011; Njome and de Wit, 2014). This volcanic chain is more than 1700 km long (Njome and de Wit, 2014) and 100 km wide (Tchoua, 1974) and can be subdivided into an oceanic and a continental segment. The oceanic part (ca. 700 km long) consists of the volcanic islands of Bioko, Principe, Sao Tome, and Annobon in the Gulf of Guinea, with two guyots located between Bioko and Principe and between Principe and Sao Tome (Burke, 2001; Njome and de Wit, 2014; Lenhardt and Oppenheimer, 2014) (Fig. 1). The continental sector of the CVL (ca. 1000 km long) (Njome and de Wit, 2014; Lenhardt and Oppenheimer, 2014) is characterised by more than 60 anorogenic plutonic complexes, monogenetic volcanoes of variable sizes and shapes, large polygenetic stratovolcanoes, and even calderas (Kagou et al., 2010; Marzoli et al., 2015; Gountié Dedzo et al., 2019).

The Kapsiki Plateau represents the CVL's northernmost part, which is in Cameroon's administrative Far North Region. Due to a lack of comprehensive research, its petrogenetic evolution remains largely unknown. The Kapsiki Plateau rises to an average altitude of 800 m. It has an area of ca. 150 km^2 and is host to a variety of different volcanic complexes (Nformida-Ndah et al., 2022). The Kapsiki Plateau's volcanic activity is distinct from other CVL' volcanoes by the relative abundance of felsic and intermediate over basaltic rocks (Ngounouno et al., 2000; Tamen et al., 2015; Gountié Dedzo et al., 2019; Tchouhla et al., 2023). The prominent volcanic plugs of the area are aligned in three directions (N30°E, N65°E, and N165°E) that line up with the CVL, the Adamawa Shear Zone, and the Benue Trough (Fig. 1b), i.e., the three major regional trends well-known in the Precambrian basement (Regnoult, 1986). Considering both the regional lineaments and the ages of volcanism (35-27 Ma) (Vincent and Armstrong, 1973; Dunlop, 1983; Ngounouno et al., 2000, 2008), it is proposed that the volcanic activity on the Kapsiki Plateau resulted from a singular resurfacing phase in the Neogene, driven by the north-eastward displacement of the African plate (Ngounouno et al., 2000; 2008; Tamen et al., 2015).

Most of the geochemical studies that have contributed to understanding the petrological complexity of the CVL have focused on the oceanic and central continental regions (Sato et al., 1990; Ubangoh et al., 1998; Marzoli et al., 1999; Rankenburg et al., 2004, 2005; Yokoyama et al., 2007; Kamguia et al., 2008; Tchouankoue et al., 2012; Asaah et al., 2015a, b; Chako Tchamabé et al., 2015; Okomo Atouba et al., 2016; Ziem à Bidias et al., 2018; Njombie Wagsong et al., 2021). Nevertheless, some previous petrological and geochemical studies have been conducted in this northernmost part of the CVL in the southern (Ngounouno et al., 2000; 2008; Tamen et al., 2015; Nformida-Ndah et al., 2022), south-eastern (Gountié Dedzo et al., 2019), and eastern (Tchouhla et al., 2023) regions of the Kapsiki Plateau, as well as the Biu and Jos plateaus (Rankenburg et al., 2005). Despite these efforts, the northern part of the Kapsiki Plateau remains insufficiently examined. Investigating this area will enhance our comprehension of the genesis of the volcanic formations in the CVL northernmost region, shedding light on the diverse mechanisms (displacement of the African plate, plate-wide swells**,** hotspots, and hotlines, edge convection and lithospheric instability) that shaped this significant geological structure.

This research marks the inaugural presentation of extensive petrographic and geochemical data derived from the basaltic lavas of Moukoulvi, situated in the north of the Kapsiki Plateau (Fig. 1c). Notably, no earlier geochemical analysis has ever been performed on these volcanic rocks, which are among the oldest in the CVL (Vincent and Armstrong, 1973; Dunlop, 1983). The main goal of this study is to enhance our comprehension of the crystallisation process and genetic evolution of the magma, along with a discussion of their implications for the mantle source from which they originated.

2. Geological setting

Located near the equator on the western edge of Africa, the CVL is the only intraplate alkaline to transitional volcanic province that includes both continental and oceanic sectors

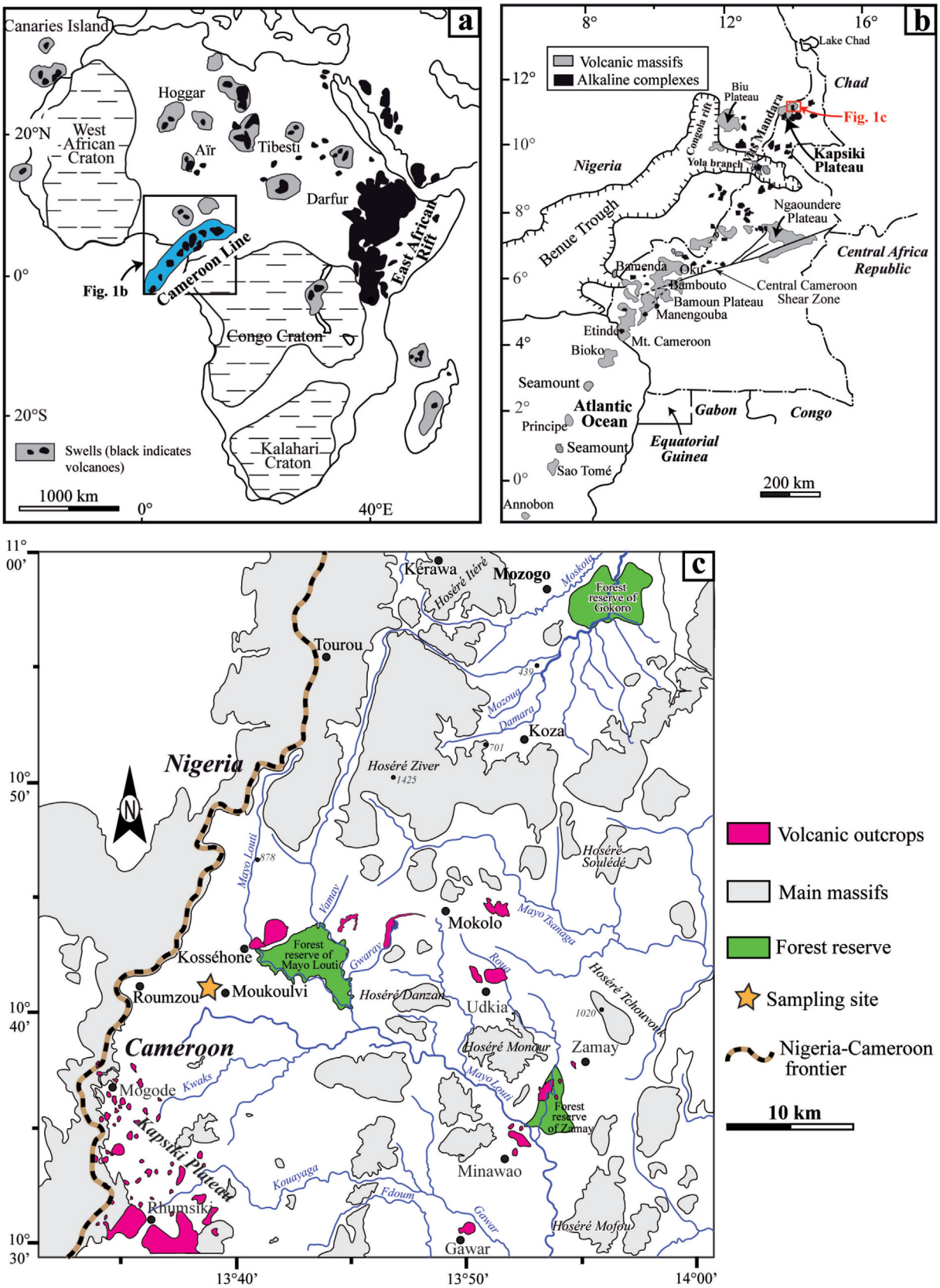

Fig. 1. a) Location map of the Cameroon Volcanic Line (CVL), indicating the main geologic features in Africa; b) The main volcanic centres and alkaline complexes of the CVL with the location of the Central African Shear Zone (CASZ); c) Simplified geological map of the Kapsiki Plateau and vicinity; volcanic outcrops are from Ngounouno et al. (2000), Tamen et al. (2015), Gountié Dedzo et al. (2019) and Tchouhla et al. (2023).

(Njome and de Wit, 2014). The Paleogene to Holocene volcanoes that make up the CVL's continental section form a Y-shaped lineament with two branches (Fitton, 1987; Njome and de Wit, 2014): one that extends east to the Adamawa (Ngaoundere) Plateau of NE Cameroon, and one that heads north into Nigeria, terminating at the Biu Plateau. Only a few volcanoes, such as Mts. Cameroon and Etinde, exhibit unimodal compositions. Other volcanoes or volcanic areas, such as the Kapsiki and Ngaoundere plateaus and Mts. Oku, Bamenda, Bambouto, and Manengouba, are bimodal (Tchouhla et al., 2023). They are composed of mafic volcanic products (basanites, basalts) and more differentiated rocks (trachytes, phonolites, rhyolites, and ignimbrites), ranging in age from 51.8 Ma (Bamoun Plateau) to the present (Mt. Cameroon) (Ngounouno et al., 2000; Moundi et al., 2007; Njome and de Wit, 2014; Ngounouno Yamgouot et al., 2018; Gountie Dedzo et al., 2019, 2020, 2022; Asaah et al., 2020; Nemzoue et al., 2020; Tchop et al., 2020; Ngwa et al., 2021).

The Kapsiki Plateau consists of three main geological units: igneous and metamorphic rocks associated with the Cameroon Pan-African chain (Toteu et al., 2001), volcanic to sub-volcanic complexes linked to the CVL (Ngounouno et al., 2000; 2008; Déruelle et al., 2007; Tamen et al., 2015; Gountie Dedzo et al., 2019; Tchouhla et al., 2023), as well as quaternary deposits from Lake Chad and the surrounding area (Adjia et al., 2013; Tsozué et al., 2017). The Kapsiki Plateau spans the Cameroon–Nigeria border and rises above a Pan-African basement of granitoids and orthogneisses that is part of the northern unit of the Cameroonian Pan-African domain. The youngest Nd and Hf TDM ages in this region, according to Bute et al. (2019), are Paleoproterozoic (1.3–2.1 Ga), which is distinct from Pan-African rocks with Archean heritage found in other Pan-African regions like the Adamawa-Yade domain (Ganwa et al., 2016). It is believed that the Mohorovicic discontinuity lies between 24 and 33 km below the surface of the Kapsiki Plateau (Poudjom Djomani et al., 1995; Tokam et al., 2010).

A small number of basaltic lava flows connected to trachyte and rhyolite plugs define the volcanic activity in the Kapsiki Plateau (Ngounouno et al., 2000). The alkaline nature of these formations has been confirmed through the analysis of olivine basalts, trachytes, trachytic breccias, and peralkaline rhyolites (Vincent and Armstrong, 1973; Gouhier and Rollet, 1978; Fitton, 1987; Ngounouno et al., 2000; Gountié Dedzo et al., 2019; Tchouhla et al., 2023). The diverse sources of these formations were highlighted, including the mantle and/or the oceanic crust (Nformida-Ndah et al., 2022). Beneath the Kapsiki Plateau, the predominant geological composition of the basement consists of migmatites and anatectites belonging to the Precambrian Mokolo Group (Ngounouno et al., 2000; 2008; Tamen et al., 2015; Tchouhla et al., 2023). These rocks are intruded by granites generated during the Pan-African orogeny (Dumort and Peronne, 1966; Toteu et al., 1987) and are covered locally by Lower Cretaceous continental sediments (less than 20 m thick sandstones, red muds, and conglomerates) (Ngounouno et al., 2000; Gountié Dedzo et al., 2019; Tchouhla et al., 2023). According to Ngounouno (1993) and Moreau et al. (1987), numerous faults that underwent reactivation during the Cenozoic era notably impacted earlier basaltic lava flows situated to the south of the Kapsiki Plateau. The dating of three basaltic lava samples from Kila using K–Ar revealed relatively consistent ages: 27.4 ± 0.5 Ma (Vincent and Armstrong, 1973), 30.41 ± 0.69 Ma, and 33.21 ± 1.33 Ma (Dunlop, 1983). Similarly, two trachytes from Gouria and Omtémalé exhibited congruent ages within acceptable error margins: 29.6 ± 0.6 Ma (Vincent and Armstrong, 1973) and 35.31 ± 2.39 Ma (Dunlop, 1983). Additionally, seven rhyolites, including one from the Mchirgui spine, yielded Rb ± Sr ages ranging between 29 and 32 ± 0.5 Ma (Dunlop, 1983).

The basaltic flow from Moukoulvi is a succession of several lobes overlying one another, between 13°39′ 00″ and 13°39′ 30″ eastern meridians and 10°40′ 50″ and 10°41′ 15″ northern parallels (Fig. 2a). These outcrops, separated by approximately 900 m, are among the more uncommon ones in the area because this region is mainly composed of felsic lavas that have received the least attention and will be the subject of a future contribution.

3. Materials and methods

For this study in the northern part of the Kapsiki Plateau, fifteen (15) rock samples from Moukoulvi were selected for geochemical analysis. The studied samples generated from several magmatic chambers overlapping one another (Fig. 2a), underwent several detailed analyses. Petrographic thin sections were made from ten of these samples. Subsequently, all the samples were finely ground using a tungsten-carbide milling pot at the University of Pretoria. This preparation was followed by X-ray diffraction (XRD) and X-ray fluorescence (XRF) analyses (Loubser and Verryn, 2008).

To conduct X-ray diffraction (XRD) analysis, the PANalytical X'Pert Pro powder diffractometer was employed, configured in a θ–θ arrangement with an X'Celerator detector. The instrument featured variable divergence and fixed receiving slits, utilising Fe-filtered Co-Kα radiation (λ = 1.789 Å). Mineralogy determination involved selecting the most fitting pattern from the ICSD database for the measured diffraction pattern, facilitated by the X'Pert_Highscore Plus software. The relative phase amounts (wt.%) were then estimated using the Rietveld method, employing the X'Pert_Highscore Plus software.

For the XRF analyses, major elements, and selected trace elements of all the samples were performed using a Thermo Fischer ARL Perform ‘X Sequential XRF instrument with OXSAS software. SARM 49 was used for quality control with an accuracy better than 1 % for the major element oxides.

At the University of Witwatersrand (WITS), trace element analysis was performed using the PerkinElmer DRC-e inductively coupled plasma mass spectrometer (ICP-MS) and analysed against certified primary solution standards. To ensure the reliability of the data, all the samples were analysed in conjunction with BCR-1, BHVO-1, and BIR-1 international reference materials (Vonopartis et al., 2020). The samples were prepared using

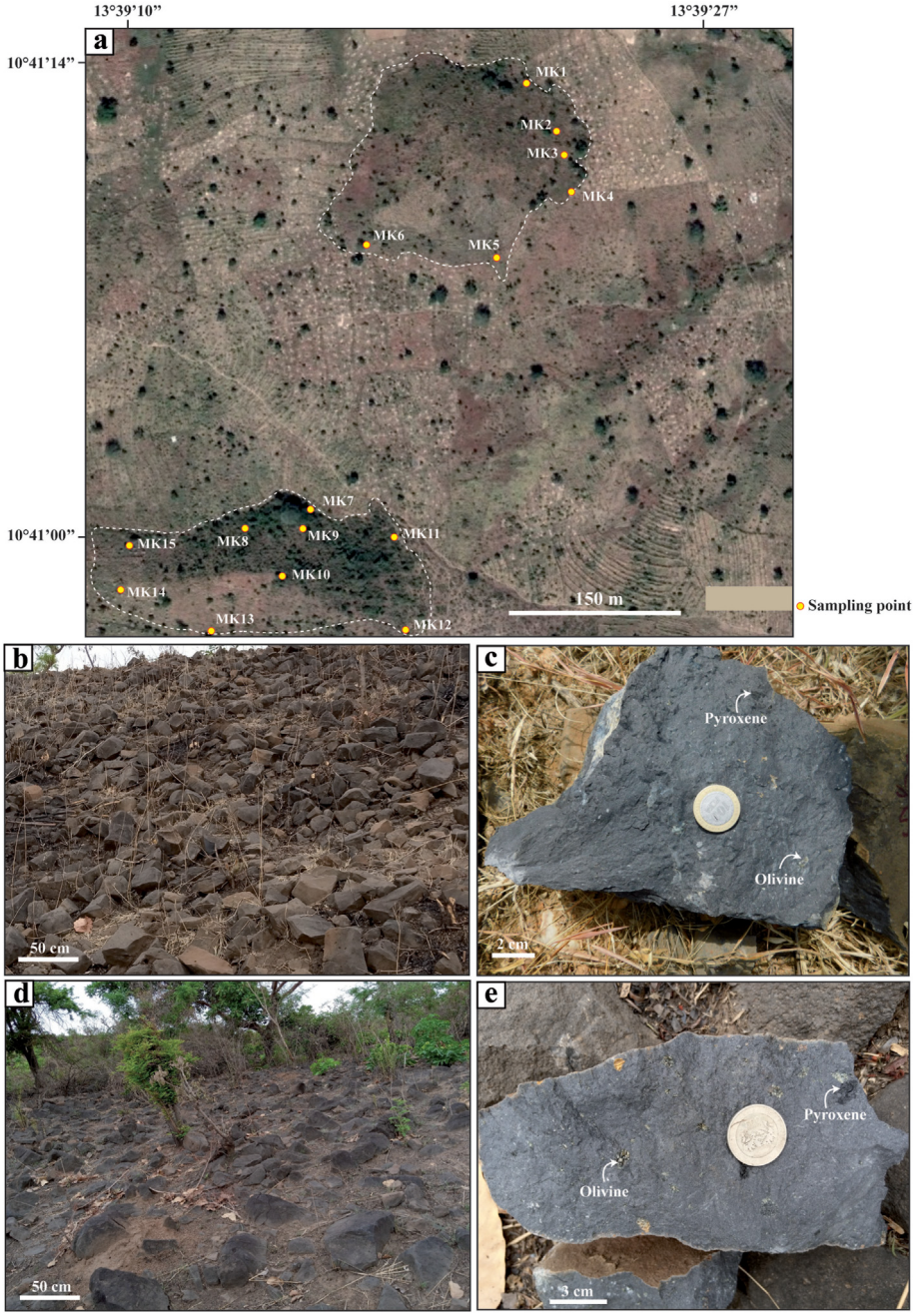

Fig. 2. (a) Google map of study area presenting the sampling point. Field photos of basalt outcrop (b) with the corresponding hand sample (c). Field photos of basanite outcrop (d) with the corresponding hand sample (e).

the CEM Mars microwave system for HF–HNO_3 digestion, and after drying, they were placed in solution with 2 % HNO_3. For ICP-MS analysis, the samples were diluted 1000 times and combined with internal Re, Rh, Bi, and In standards to provide the needed mass range. Primary external calibration standards were created in the range of 5–100 ppb. Every ICP-MS determination was accompanied by the control standards BCR-1, BHVO-1, and BIR-1. All elements deviated less than 10 % from the recommended values.

Using the PRIMELT software (Herzberg and Asimow, 2008), we were able to determine the ambient temperature [T (°C) = 935 + 33MgO – $0.37MgO^2$ + 54P – 2P] and potential mantle temperature [Tp (°C) = 1463 + 12.74MgO – 2924/MgO] of the Moukoulvi mantle source. The lavas frequently have major and trace element compositions that are similar to primitive mantle (Ni: 300–400 ppm; Cr: 300–500 ppm; Co: 50–70 ppm; Jung and Masberg, 1998). To compute the T and Tp, we used the most basic sample from (MK5: MgO = 13.69 wt%, Cr = 676 ppm, Ni = 345 ppm, Co = 71 ppm). For this most primitive sample, the computed T and Tp resulted in 1423.1C and 1545.7C, respectively.

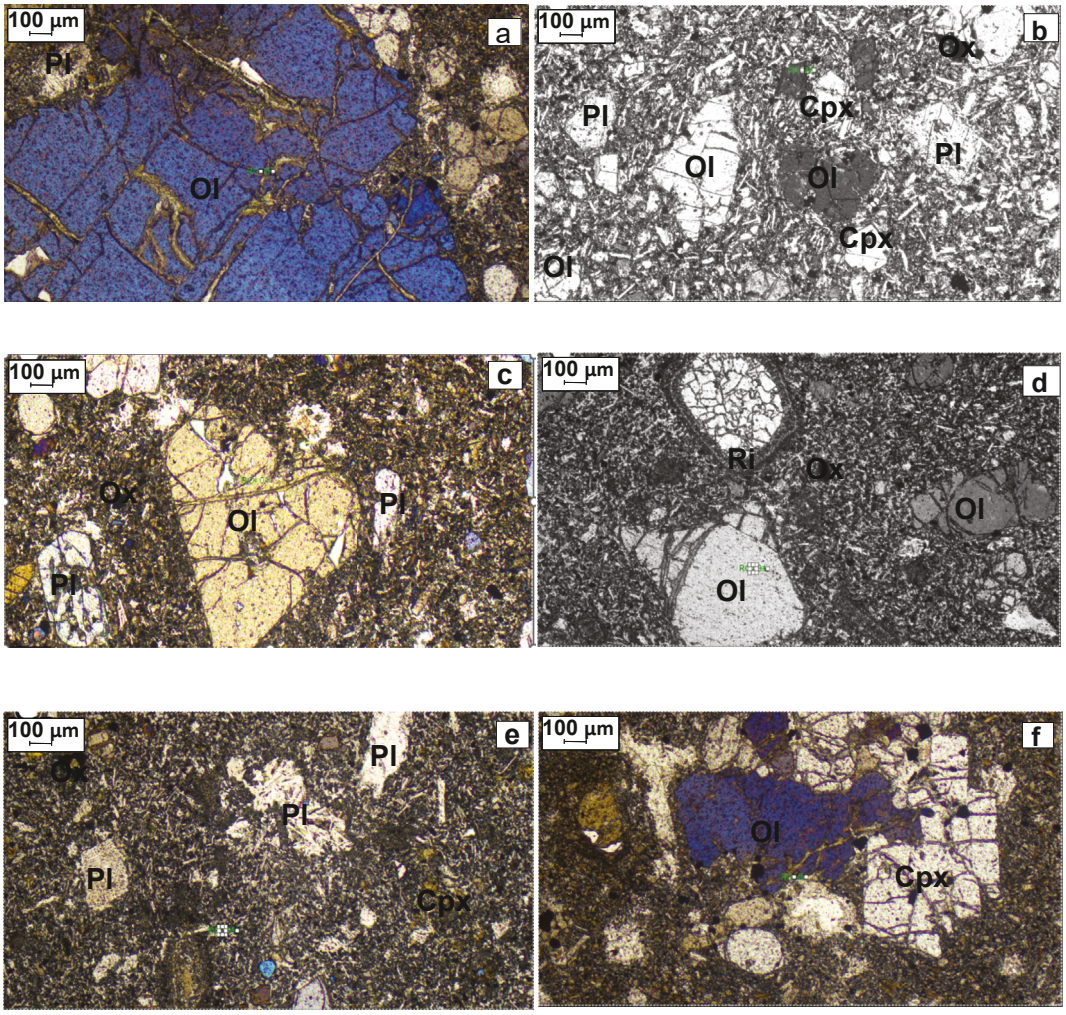

Fig. 3. Optical microphotographs of basanite and basalt in thin section. (a) Typical porphyritic texture of basanite showing olivine (Ol) phenocryst surrounded by microlites of plagioclase. (b) Clinopyroxene (Cpx), Plagioclase (Pl), Oxyde (Ox) and Ol microcysts. c): Euhedral olivine (Ol) crystals may be iddingsitized and/or corroded. (d) Quartz xenocryst with reaction rim (Ri). (e) Pl, Ol, Cpx, and Fe–Ti oxides surrounded by the groundmass. (f) Cpx with green core.

4. Results

4.1. Nomenclature and petrography

According to the silica *versus* (*vs.*) total alkali diagram (TAS; Le Bas et al., 1986) (Fig. 4), combined with the Irvine and Baragar (1971) alkaline-subalkaline dividing line, the samples are mainly basanites and basalt with an alkaline composition, similar to the majority of the rocks in the northern part of CVL. The K_2O *vs.* Na_2O diagram (Middlemost, 1975) (Fig. 4) shows that the alkaline samples belong to the Na-series (Na_2O/K_2O = 1.78–3.47).

The basanites and basalts from the Moukoulvi volcanoes predominantly occur as decimetric to metric blocks at the surface (Fig. 2b–d). The size of the rocks varies from the bottom to the top, with larger blocks being covered by smaller pieces. The rocks have a dark colour (mesocratic to melanocratic) with a compact structure and a microlithic porphyritic texture. They contain large olivine and clinopyroxene phenocrysts with some rare plagioclase, as well as the basement enclaves that are large enough to be identified without a microscope.

Olivine occurs as phenocrysts and microcrystals, representing about 40 % of the volume of the rock. The larger phenocrysts range from 0.4 × 0.7 mm to 0.3 × 0.5 mm. The smaller phenocrysts are about 0.1 × 0.2 mm to 0.15 × 0.1 mm. They have a limpid or light whitish colour in PPL (plane polarised light) (Fig. 3b–d) and a blue or yellow colour in XPL (cross polarised light) (Fig. 3a–c, f). We also noticed a few irregular cracks intruded by oxide inclusions and pyroxene microcrystals (Fig. 3a–c, d). Some of the crystals are corroded and reabsorbed by the groundmass and exhibit vesicles formed during the crystallisation (Fig. 3e). Some olivine presents evidence for iddingsitization (Fig. 3a–c). Plagioclase occurs as microcrystals that may form up to 25 % of the rock in the form of small prisms and are elongated into sub-rounded shapes that range from 0.3 × 0.1 mm to 0.2 × 0.03 mm long and 0.07 × 0.02 mm to 0.05 × 0.01 mm wide (Fig. 3b, c, d). Pyroxenes have a proportion of about 15 % with automorphic to subautomorphic shapes, which range from 0.6 × 0.3 mm to

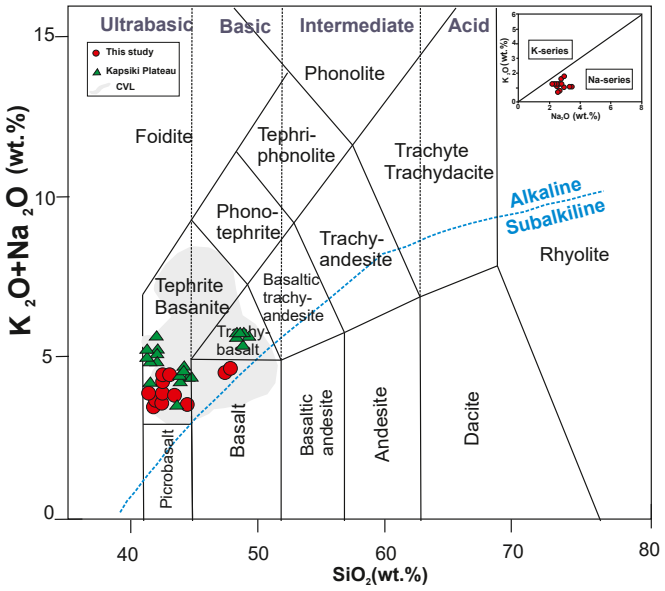

Fig. 4. Total alkali *vs.* silica classification diagram (after Le Bas et al., 1986); Inset: Na_2O *vs.* K_2O subdivision diagram of the alkaline series (Middlemost, 1975). The alkaline-subalkaline dividing line is from Irvine and Baragar (1971). Literature data from the Kapsiki Plateau (Ngounouno et al., 2000; Gountié Dedzo et al., 2019; Tchouhla et al., 2023) and other CVL data are also displayed for comparison. Bamboutos (Kagou et al., 2010; Marzoli et al., 2015; Merle et al., 2017); Ngaoundere (Nkouandou et al., 2008; Nkouandou and Temdjim, 2011; Tiabou et al., 2019; Njombie Wagsong et al., 2021; Mebara Onana et al., 2022); Mount Cameroon (Tsafack et al., 2009; Wandji et al., 2009; Ngounouno Yamgouot et al., 2018); Mount Oku (Konfor et al., 2007; Chenyi et al., 2017); Bamenda (Kamgang et al., 2013); Bamoun (Okomo Atouba et al., 2016; Ziem à Bidias et al., 2018) Tombel graben (Nkouathio et al., 2008) and Bafang (Tchuimegnie Ngongang et al., 2015; Ngongang Tchikankou et al., 2020).

0.4 × 0.2 mm in length and a width of about 0.5 × 0.2 mm to 0.3 × 0.2 mm, exhibiting a white colour in PPL (Fig. 3b) and a light grey colour in XPL (Fig. 3b–f). They may occur as inclusions in olivine and exhibit a two-directional cleavage only in the basal section (Fig. 3a–c).

The groundmass consists of plagioclase, olivine, clinopyroxene, and Fe–Ti oxides. Quartz xenocrysts with wavy extinction jacketed by clinopyroxene coronas and alkali feldspar with disequilibrium textures occasionally occur in the basanites (Fig. 3d). Some samples contain clinopyroxenes with green cores (MK1, MK5; Fig. 3f).

4.2. Whole rock geochemistry

The major element oxide (wt%) and trace (ppm) elements data for the fifteen representatives Moukoulvi samples are presented in Table 1. The samples display relatively low LOI values (1.33–2.14 %) and no obvious signs of alteration. Hence, they were all considered for data analysis.

CaO remains nearly constant for the studied samples with MgO >11wt%, revealing the absence of a correlation between CaO and MgO, whereas the SiO_2 content shows strong negative correlations with MgO (Fig. 5). The Fe_2O_3 contents are high (10.94–12.73 wt%) and correlate positively with increasing MgO, in contrast to the other samples of the CVL (Fig. 5). Their Al_2O_3 contents (12.17–14.05 wt%) correlate negatively with MgO (Fig. 5). The CaO/Al_2O_3 ratios vary within a relatively narrow range (0.65–0.91) and correlate positively with MgO, as those in other lavas of the CVL (Fig. 5). There is a positive correlation between CaO/Al_2O_3 and MgO as well as between Cr and MgO for the samples with MgO < 12 wt%. The CaO/Al_2O_3 ratios remain nearly constant for the samples with MgO > 12 wt%. The lavas also have relatively high Na_2O contents (2.2–3.3 wt%) with low P_2O_5 (0.71–0.83 wt%) and K_2O varying from 0.75 to 1.65 wt%.

Ni concentrations range from 176 to 344 ppm, while the Cr content varies from 282 to 680 ppm. Ni and Cr exhibit a relatively strong positive correlation with MgO (Fig. 6), indicating their compatibility. In contrast, Rb, Ba, Sr, Zr, Y, La, and Ce show no clear correlation with MgO (Fig. 6). Sr and Rb display a slight fluctuation with MgO and relate to mafic lavas found in other volcanic centres of the Kapsiki Plateau.

The chondrite-normalised REE patterns (Fig. 7a) show the fractionation of light rare earth elements (LREEs) in relation to heavy REE rare earth elements (HREEs) (La_N/Yb_N = 19.55–22.86) highlighted by negative slopes and characterized by enrichment in LREEs and depletion in HREEs. The REE concentrations in the studied samples are generally lower than those of the CVL and Kapsiki Plateau lavas. There is no Ce anomaly in Moukoulvi samples compared to generally positive Ce anomaly for Kapsiki Plateau lavas. The samples plot above Normal Mid-Ocean Ridge Basalts (N-MORB) and Enriched Mid-Ocean Ridge Basalts (E-MORB) and are very close to that of Ocean Island Basalt (OIB). This observation shows that the lavas in the study area are more enriched in REEs than N-MORB and E-MORB.

In the primitive mantle-normalized patterns, the samples are roughly comparable to those of OIB. However, the studied lavas have LILE contents (Sr = 812–1065 ppm, Ba = 394–467 ppm) that are relatively high compared to average OIB (Sr = 660 ppm, Ba = 350 ppm; Sun and McDonough, 1989). They are more enriched in LILE relative to HFSE (Sr/Zr = 3.97–4.94, average OIB = ~1; Ba/La = 9.42–11.72, average OIB = 9.4) and have Zr/Sm ratios (26.93–29.88) that are similar to average OIB (Zr/Sm = 28) (Sun and McDonough, 1989). The profiles of the samples are more enriched in trace elements than those of N-MORB and E-MORB. There is no depletion of Nb and Ta on the spider diagrams (Fig. 7b) and the samples have low U (1.48–1.81 ppm) concentrations. Significantly low Cs/Rb (0.005–0.01) ratios are direct consequence of low Cs contents. According to Hofmann et al. (1986) and Sun and McDonough (1989), the Nb/U (37.3–51.6) and Nb/Ta (19.04–20.08) ratios are both high and fall within the OIB (Nb/Ta = 17 ± 2) field.

5. Discussion

5.1. Crustal contamination

It is crucial to assess the potential impacts of crustal contamination that might have impacted the ascending magmas given the continental setting in which the alkaline mafic lavas

Table 1
Major (wt.%) and trace (ppm) element data for the Moukouvlvi lavas.

Rock type	basanite	basanite	basanite	basanite	basanite	basanite	basanite	basalt	basalt	basanite	basanite	basanite	basanite	basanite	basanite
Sample ID	MK1	MK2	MK3	MK4	MK5	MK6	MK7	MK8	MK9	MK10	MK11	MK12	MK13	MK14	MK15
Lon E	13°39'21.9″	13°39'22.72″	13°39'22.9″	13°39'23.4″	13°39'20.6″	13°39'17.1″	13°39'15.9'	13°39'13.96″	13°39'15.6″	13°39'14.9″	13°39'18.3″	13°39'17.9″	13°39'12.9″	13°39'10.5″	13°39'10.5″
Lat N	10°41'13.5″	10°41'12.02″	10°41'11.31″	10°41'10.1″	10°41'8.4″	10°41'8.7″	10°41'1.2″	10°41'00.8″	10°41'00.5″	10°40'59.3″	10°41'00.1″	10°40'57.4″	10°40'56.6'	10°40'58.81″	10°41'00″
SiO2	41.41	41.1	41.02	40.56	41.31	40.59	40.48	46.58	46.48	42.51	42.09	42.31	41.92	43.31	42.26
Al2O3	12.72	12.26	12.6	12.17	12.3	12.19	12.24	14.05	14.01	13.82	13.75	13.84	13.51	13.78	13.78
Fe2O3	12.26	12.26	12.31	12.73	12.22	12.71	12.72	11.11	10.94	11.73	11.77	12.07	11.82	11.68	12.01
MgO	12.97	13.64	12.76	13.35	13.69	13.37	13.47	9.87	9.85	11.94	11.84	11.43	11.87	11.23	11.41
CaO	10.27	10.42	10.19	10.55	10.13	10.73	10.63	8.63	8.57	10.52	10.25	10.38	10.44	10.15	10.5
Na2O	3.23	2.46	3.29	2.73	2.94	2.65	2.59	2.79	2.83	2.52	3.3	2.45	2.74	2.2	2.33
K2O	0.99	1.07	1.02	1.04	0.92	0.8	0.75	1.65	1.65	1.26	1.02	1.27	1.13	1.23	1.27
TiO2	3.06	3.04	3.04	3.19	2.98	3.24	3.22	2.53	2.5	2.91	2.84	2.93	2.88	2.76	2.92
P2O5	0.81	0.76	0.8	0.81	0.75	0.81	0.81	0.73	0.71	0.8	0.83	0.79	0.82	0.78	0.79
MnO	0.19	0.19	0.18	0.19	0.19	0.19	0.2	0.17	0.16	0.17	0.18	0.2	0.17	0.17	0.2
LOI	1.35	2.08	2.14	1.97	1.97	2.06	2.29	1.33	1.76	1.18	1.56	1.69	2.04	2.12	1.87
Total	99.98	99.98	99.98	99.98	99.98	99.94	99.98	99.98	99.96	99.98	99.99	99.95	99.97	99.97	99.95
Mg#	67.7	68.8	67.3	67.5	68.9	67.6	67.7	63.8	64.1	66.9	66.6	65.2	66.6	65.6	65.3
Cs	0.53	0.50	0.52	0.52	0.56	0.52	0.49	0.75	0.77	0.35	0.49	0.38	0.59	0.56	0.45
Rb	59.10	91.64	60.31	51.37	66.61	48.38	34.91	50.13	50.09	36.62	41.69	38.98	62.06	35.74	39.67
Ba	440.50	418.72	450.59	425.40	422.32	414.04	445.58	467.66	453.59	424.74	429.86	397.70	424.62	394.53	397.65
Sr	913.50	860.48	891.61	927.17	851.43	897.04	869.03	812.44	820.53	1017.88	951.20	1065.58	986.07	934.10	1027.56
Pb	1.67	1.82	1.55	1.59	1.65	1.80	1.68	3.30	3.31	1.73	2.05	1.50	1.68	1.78	1.64
Th	5.30	4.92	5.42	4.95	5.20	4.72	4.83	5.94	5.90	5.19	5.71	5.07	5.44	5.06	5.05
U	1.65	1.52	1.70	1.57	1.59	1.48	1.51	1.82	1.65	1.63	1.76	1.57	1.68	1.55	1.56
Zr	222.83	208.82	221.87	216.77	209.08	212.98	214.10	203.72	206.56	206.64	220.97	207.53	215.43	201.99	207.90
Hf	4.70	4.50	4.83	4.68	4.55	4.71	4.64	4.62	4.57	4.42	4.62	4.49	4.59	4.50	4.46
Ta	4.28	3.95	4.27	3.95	4.01	3.77	3.96	3.58	3.52	4.12	4.32	4.01	4.22	3.82	4.06
Y	20.52	19.82	20.61	20.82	19.67	20.72	20.79	18.20	18.30	18.74	19.69	18.88	19.59	18.06	18.61
Nb	84.59	78.56	84.73	77.80	78.90	75.38	77.64	67.96	68.19	80.55	86.84	79.27	84.24	72.83	77.98
Sc	24.91	25.10	24.02	25.33	24.09	25.19	24.81	19.24	19.33	22.94	22.94	22.91	23.06	22.20	22.25
Cr	657.17	680.66	637.78	641.86	676.26	638.07	653.63	286.37	282.89	496.60	483.08	476.27	511.83	392.24	469.90
Ni	303.24	324.88	290.14	290.80	344.67	287.06	301.32	176.52	178.41	246.27	252.75	236.92	249.03	205.25	235.59
Co	68.70	74.22	65.31	64.97	71.71	72.77	73.21	58.98	56.01	69.76	62.62	59.98	61.19	58.28	58.19
V	274.58	279.15	276.65	292.19	276.10	298.08	291.67	230.01	227.34	276.03	266.49	278.88	268.88	263.90	275.17
Ga	20.88	19.45	20.53	19.92	19.65	19.85	19.77	20.73	20.53	20.28	21.02	20.45	20.53	19.87	20.32
Zn	114.27	103.12	101.30	103.01	96.74	103.39	103.16	96.73	97.12	102.55	102.29	98.64	100.12	96.62	98.65
Cu	91.38	83.33	67.00	79.99	80.47	79.20	81.37	57.32	57.36	93.23	71.34	77.81	72.10	68.79	69.48
La	43.84	41.22	44.54	42.08	41.50	41.75	41.57	39.88	39.59	43.50	45.62	41.98	44.38	40.26	42.20
Ce	83.08	78.25	85.43	80.91	79.64	80.41	81.54	76.31	75.66	82.44	86.20	79.39	83.36	77.38	80.01
Pr	9.71	9.16	9.94	9.53	9.24	9.50	9.36	8.81	8.63	9.39	9.83	9.11	9.61	8.81	9.13
Nd	40.07	37.92	40.19	39.98	38.10	39.66	39.21	35.96	35.13	38.18	39.52	37.16	38.77	36.32	37.43
Sm	7.72	7.45	7.92	7.77	7.48	7.91	7.90	6.97	6.91	7.23	7.51	7.17	7.39	7.01	7.21
Eu	2.57	2.48	2.62	2.63	2.49	2.64	2.64	2.31	2.28	2.44	2.50	2.41	2.48	2.32	2.39
Gd	6.84	6.71	7.04	7.04	6.68	7.13	7.13	6.27	6.11	6.53	6.68	6.46	6.55	6.26	6.42
Tb	0.86	0.85	0.89	0.89	0.85	0.90	0.91	0.79	0.78	0.82	0.84	0.82	0.83	0.79	0.81
Dy	4.53	4.45	4.67	4.72	4.46	4.71	4.76	4.16	4.12	4.30	4.37	4.27	4.33	4.17	4.20

Ho	0.79	0.77	0.80	0.82	0.76	0.82	0.82	0.73	0.72	0.74	0.76	0.75	0.74	0.73	0.73			
Er	1.92	1.88	1.96	1.97	1.87	1.98	1.99	1.81	1.79	1.83	1.87	1.80	1.84	1.76	1.78			
Tm	0.25	0.24	0.25	0.25	0.24	0.25	0.25	0.23	0.23	0.23	0.23	0.23	0.23	0.23	0.23			
Yb	1.49	1.45	1.52	1.53	1.45	1.53	1.52	1.45	1.42	1.41	1.43	1.41	1.40	1.38	1.40			
Lu	0.21	0.20	0.21	0.21	0.20	0.21	0.21	0.20	0.20	0.19	0.20	0.19	0.20	0.19	0.19			

Mg# = molar ratio of [MgO/(MgO + FeO)] x 100).

of the Kapsiki Plateau erupted. For example, the Mokolo-Kossehone mafic lavas (Tchouhla et al., 2023) of the Kapsiki Plateau are a good example of the crustal contamination processes linked to the differentiation of the magmas (AFC process), which have already been noted in the other volcanic massifs of the CVL (Halliday et al., 1988; Marzoli et al., 2000; Rankenburg et al., 2005; Kamgang et al., 2007; 2013). One method to monitor crustal contamination is by analysing major and trace elements that could be influenced by the Pan-African granites, which have high SiO_2 content (Marzoli et al., 2000). When plotted against SiO_2 the decrease in incompatible element contents (Th, La, and U) (Fig. 8a) can, for instance, can be attributed to contamination by crustal rocks. The samples should subsequently exhibit a correlation between their U, Th, La, and SiO_2 concentrations (Nicholson et al., 1991), as these elements are more abundant in the crust than in mantle magmas. Given that they are indicative of the crust's geochemical signature, they are enriched because of magma interaction or absorption of continental crust components, according to the correlations found. This interpretation is further supported by the Nb/Y *vs.* Rb/Y diagram (Fig. 8b), which shows the samples represented as a comparatively flat trend in the examined samples, such as the Precambrian basement samples. The relatively flat trend observed in the studied samples suggests a possible connection to assimilation fractional crystallisation (AFC) processes as evidence by the presence of the basement enclaves in the studied samples (Fig. 3).

5.2. Fractional crystallisation

Like many other lavas from the Kapsiki Plateau, the basaltic lavas from Moukoulvi display major and trace elements that follow typical differentiation patterns. Their Ni (176–344 ppm) and Cr (282–680 ppm) contents are lower than what is expected for pure mantle melt crystal fractionation of a primary magma (Ni > 400 ppm, Cr > 1000 ppm; Frey et al., 1978) and instead coincide with fractionation occurring during magma ascent. Nickel is generally a sensitive indicator of olivine fractionation or accumulation in basaltic magma because of its large partition coefficient (Saadat et al., 2010). In addition, decreasing concentrations of Cr and Ni related to decreasing MgO correspond to the fractionation of olivine and clinopyroxene. There is a clear positive correlation between CaO/Al_2O_3 and MgO values of 12 wt%, implying that clinopyroxene fractionation play a significant role during the early stages of magma evolution. Thus, the positive correlation between CaO/Al_2O_3, Cr, and MgO < 12 wt% suggests the fractional crystallisation of clinopyroxene (Green, 1980). Therefore, the changing pattern at around 12 wt % MgO reflects a change in fractionation from olivine alone to olivine + clinopyroxene. This suggests that clinopyroxene fractionation was limited, which is consistent with the scarcity of clinopyroxene phenocrysts in the studied samples and elsewhere in the CVL (Njombie Wagsong et al., 2021).

The negative correlations between Al_2O_3 and MgO (Fig. 5) and the positive correlation between Sr and MgO (Fig. 6) for the studied samples argue against plagioclase fractionation,

which is consistent with the absence of plagioclase phenocrysts. Sr does not show a negative anomaly, indicating that it behaved incompatibly within the magma. The absence of a negative Eu anomaly further suggests that low-pressure plagioclase fractionation was minimal or absent. The decrease in TiO_2 and Fe_2O_3t with decreasing MgO indicates fractionation of Fe–Ti oxides (Fig. 5).

As a result, the studied lavas' major fractionation assemblage is olivine + clinopyroxene + Fe–Ti oxide. Thus, during the process of magma crystallisation, minerals containing iron and magnesium incorporate trace elements such as Sc, Cr, Ni, and Co that are compatible with their structure (Wilson, 1992). As the magma evolves, these ferro-magnesian minerals like olivine, clinopyroxene, and ferrotitanium oxide separate out, leading to a reduction in the concentration of these elements.

5.3. Mantle source and melting

The mafic rocks of the Moukoulvi area vary in both major and trace element compositions (Figs. 5 and 6), which are strongly correlated with their MgO content. Due to their relatively higher enrichment in LREE compared to HREE, the lavas undergo melting at depths corresponding to the stability field of garnet. The elevated Sr levels (812–1065 ppm) and comparatively lower Rb contents (34.9–268.9 ppm) closely resemble those found in both the oceanic and continental sectors of the CVL (Asaah et al., 2021). With their increased LREE levels and relative enrichment in HFSE, the examined samples have some geochemical similarities to sodic alkaline continental magmas from the CVL. However, the measured La/Nb > 0.5 is unusual for OIB, which typically have lower La/Nb values. The incompatible element patterns of the Moukoulvi lavas align with the OIB pattern (Fig. 7b), a characteristic also observed in most volcanic centres of the CVL. Consequently, the presence of melts from shallower depths with residual spinel cannot be entirely dismissed for the less enriched basalts, while an enriched mantle source is deemed necessary for at least the basanites (Kamgang et al., 2013; Merle et al., 2017; Gountié Dedzo et al., 2019). The persistence of residual garnet leads to a depletion of HREE in relation to LREE due to the strong retention of HREE in garnet, as highlighted by the high partition coefficients of these elements in the mineral (Green et al., 1989; Jenner et al., 1994). This theory is further supported by the fact that similar lavas can be found along the CVL at different places (Marzoli et al., 2000; Temdjim et al., 2004; Bilong et al., 2011; Tchouankoue et al., 2012; Asaah et al., 2015a; Tiabou et al., 2018). These data suggest that the chemical anomalies are related to the original mafic magmas' composition and, consequently, the mantle source's composition (Kamgang et al., 2013). The elevated Sr and Ba contents in Moukoulvi lavas, along with their relatively low Zr contents (Fig. 7b), position them as potential contributors to the genesis of high-Sr mafic magmas.

While the MREE/HREE ratios show how much garnet is still present in the source, the LREE/HREE ratios are very sensitive to the melting (Yokoma et al., 2007). In the La/Sm plot (Fig. 9), the Moukoulvi lavas are positioned at higher Sm/Yb and La/Sm ratios. The higher Sm/Yb and La/Sm levels point to a deeper magma origin. According to Suh et al. (2003) and Asaah et al. (2015a), variations in the composition of trace elements also point to heterogeneities in the mantle sources. We used the La/Sm *vs.* Sm/Yb plot (Fig. 9) to estimate the source's mineralogy and partial melting extent. Since La and Sm are incompatible trace elements with ratios that rarely change during melting, the La/Sm ratio serves as an indicator of the degree of partial melting (Asaah et al., 2021). The reaction of Sm/Yb is affected by the mineralogy of the source (garnet/spinel), since garnet preferentially fractionates Yb (HREE) over Sm (LREE) (Asaah et al., 2021). According to melt curves for garnet and spinel lherzolites, the estimated amount of partial melting for Moukoulvi lavas suggests less than 2 % partial melting from a source with less than 4 % garnet (Fig. 9). These lavas match other CVL lavas (e.g., $(Sm/Yb)_N$ and $(Dy/Yb)_N > 1$) and exhibit steep patterns of HREE depletion, indicating the presence of residual garnet in the source (Asaah et al., 2020).

5.4. Geodynamic setting

Except for the magmatism in the East African rift, which is generally alkaline (Furman et al., 2007), magmatism linked with continental rifting is primarily thought to be tholeiitic (Sebai et al., 1991; Harry et al., 1992). The tholeiites of the CVL were most likely formed from an asthenospheric source during a period of lithospheric thinning between the Santonian and Eocene (Coulon et al., 1996). However, the alkaline rocks of the CVL may have come from a deeper metasomatized mantle source (Cantagrel et al., 1978; Dunlop and Fitton, 1979; Dunlop, 1983; Halliday et al., 1990, 1998). According to Sibuet and Mascle (1978), the CVL and the Adamawa fracture zone represent a well-fitted continental prolongation of the ascension fracture zone that occurred when the South Atlantic Ocean opened (Ngounouno et al., 2000). Several geochemical events associated with basaltic rocks are connected to the Atlantic's opening (Tchouankoue et al., 2012). The fracture zones of the Atlantic Ocean are the extension of Pan-African faults that existed on both the African and South American continents prior to the breakup of Gondwana (Cornacchia and Dars, 1983; Ngounouno et al., 2000). For the CVL, this has been described as a result of the interaction between an ascending plume component and the lithosphere (Halliday et al., 1990; Coulon et al., 1996). Beginning at around 70 Ma, Mesozoic to Early Cenozoic magmatism was replaced by CVL magmatism, which was succeeded by alkaline volcanism (Dunlop, 1983; Halliday et al., 1998). According to Fitton (1980), the similarities in "Y" form and size between the Benue Trough and the CVL (Fig. 1b) indicate that they were related to the same hot zone in the asthenosphere through which the African plate migrated to establish the rift system (Coulon et al., 1996). As evidenced by the Biu Plateau basalts (Coulon et al., 1996; Rankenburg et al., 2005), the lava originating from the northwestern branch of the Y-shaped CVL (comprising alkaline basalts, trachytes, and phonolites) was deposited in the

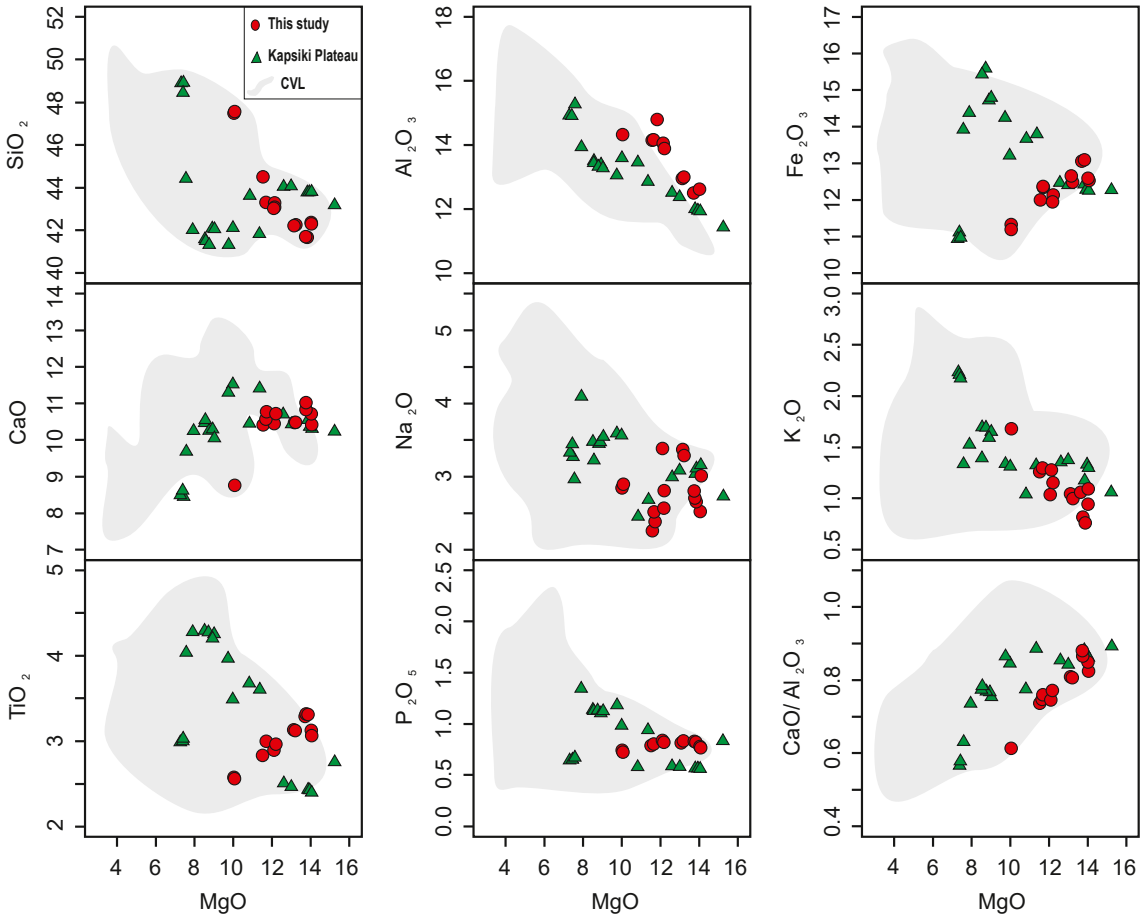

Fig. 5. Major element oxide variation diagrams of the studied samples plotted against MgO (wt.%). All samples are plotted on an anhydrous basis.

northern extremity of the Benue Trough between 23 and 7 million years ago and from 3 million years ago to the present (Grant, 1972; Guiraud, 1990). The basanites of the continental section of the CVL have fairly comparable geochemical characteristics and lack any obvious signs of contamination of the crust (Fitton, 1987; Ngounouno et al., 2000; Konfor et al., 2007; Tamen et al., 2007; Nkouathio et al., 2008; Nkouandou et al., 2008; Tsafack et al., 2009; Wandji et al., 2009; Kagou et al., 2010; Nkouandou and Temdjim, 2011; Kamgang et al., 2013; Marzoli et al., 2015; Tchuimegnie Ngongang et al., 2015; Okomo Atouba et al., 2016; Chenyi et al., 2017; Merle et al., 2017; Tiabou et al., 2018; Ziem à Bidias et al., 2018; Ngounouno Yamgouot et al., 2018; Gountié Dedzo et al., 2019; Ngongang Tchikankou et al., 2020; Njombie Wagsong et al., 2021; Mebara Onana et al., 2022; Tchouhla et al., 2023). Nevertheless, the presence of muscovite in thin sections (Fig. 3) demonstrates the chemical evidence of interaction with weathering conditions or hydrous mineral phases. It occurs in silica-rich basaltic varieties, especially in highly developed magmas linked to late-stage crystallisation or crustal contamination, and is more likely to be secondary, forming during alteration processes (Rollinson, 1993). The studied lavas, like most of the other CVL basanites and basalts, exhibit a positive K anomaly with a negative Ba anomaly on the multi-element normalised diagram (Fig. 7b). This can be explained by the occurrence of hydrous mineral phases such as phlogopite and amphibole, which have high K/Ba, K/Rb, and Ba/Rb ratios, highlighting the influence of metasomatism (Gountié Dedzo et al., 2019). Hydrous minerals could be present, suggesting the potential occurrence of modal metasomatism, as inferred from the major and trace element compositions. Elevated Rb/Sr ratios or high K_2O levels may cause the presence of hydrous phases, which are residues of modal metasomatism and include phlogopite or amphibole (Rooney et al., 2014). Phlogopite and amphibole form by infiltration and metasomatization of peridotite by volatile-rich fluids or melts from subduction or asthenospheric sources (Foley, 1992). Their stability at mantle depths influences water distribution and transport, reducing the melting temperature of neighbouring mantle rocks and causing partial melting. This process, also described as intra-mantle metasomatism (Rooney et al., 2014; Rooney, 2017), is the cause of the HIMU signature for the rocks of the East African Rift System (Rooney et al., 2020; Albino and Biggs, 2021). As a result, a small fraction of the asthenosphere melts, enriched in highly incompatible trace elements, “fossilised” in the upper non-convective mantle (Halliday et al., 1995; Asaah et al., 2020). The Moukoulvi lavas exhibit significant concentrations of incompatible trace elements (Rb, Pr, U, and Th) in comparison to average OIBs, enriched mid-ocean ridge basalts

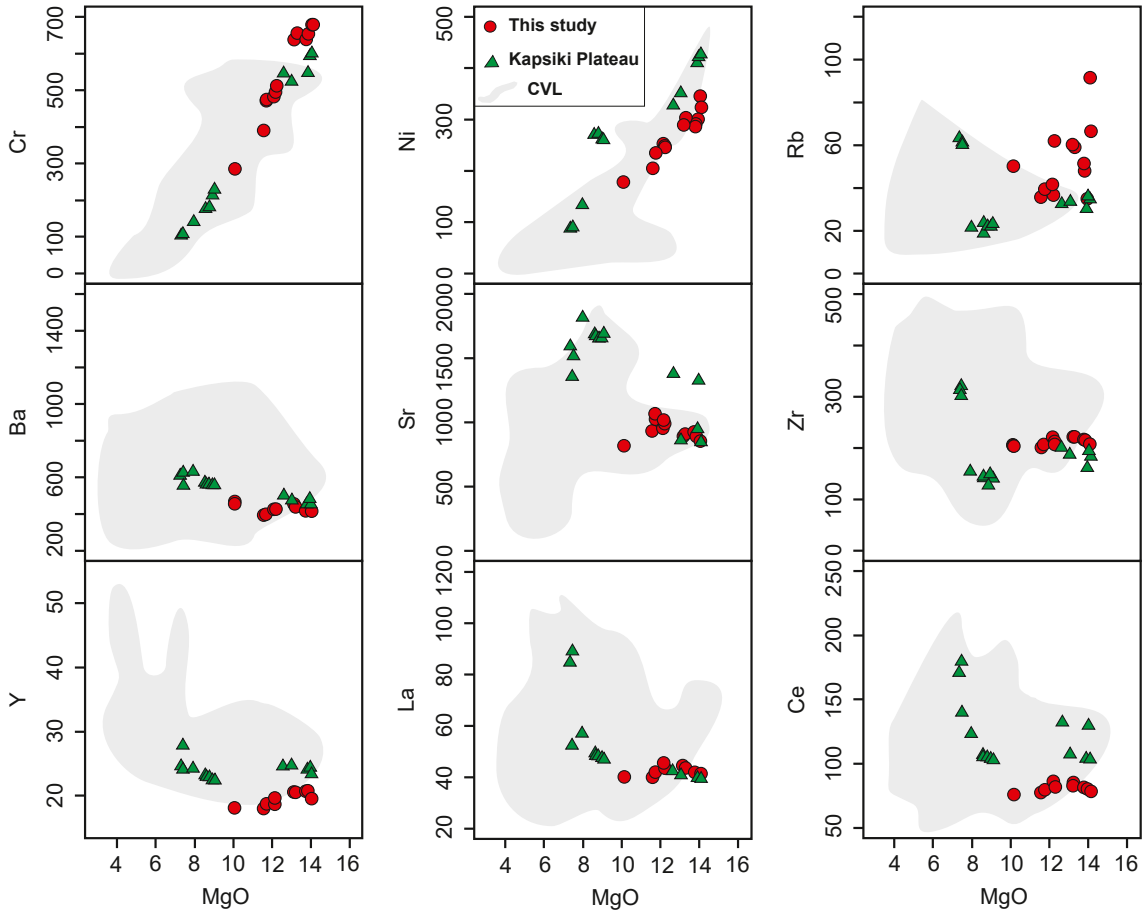

Fig. 6. Trace element (ppm) variation diagrams of the studied samples plotted against MgO (wt.%). All samples are plotted on an anhydrous basis.

(E-MORB), primitive mantle (PM), and normal mid-ocean ridge basalts (N-MORB) (Fig. 7b), indicating the presence of an enrichment event. The Moukoulvi lavas have slightly higher Ta/Yb and Th/Yb ratios than usual OIB values (Fig. 10a), as well as higher Zr/Hf and Nb/Ta (Fig. 10a) showing that they are roughly different from typical OIB magmas. OIBs have limited Nb/U and Ta/U ranges because Nb, Ta, and U have the same bulk partition coefficients (Asaah et al., 2020). This indicates that Nb and Ta are not frequently separated from neighbouring elements (U and La) by mantle melting (Hofmann, 2003; Asaah et al., 2020). It is therefore possible that other factors than partial melting contributed to the enrichment of Nb and Ta compared to U and La in the lavas (Willbold and Stracke, 2006). The Nb/Ta (19–20) and Zr/Hf (44–47) ratios of the Moukoulvi lavas vary substantially (Fig. 10b). The Nb/Ta ratios are super-chondritic compared to the Zr/Hf ratios, which exhibit a wider variation. Metasomatism is typically associated with an enrichment in highly incompatible elements such as Rb, Ba, Ce, Nb, and Zr, indicating that the asthenosphere is not the only source of these

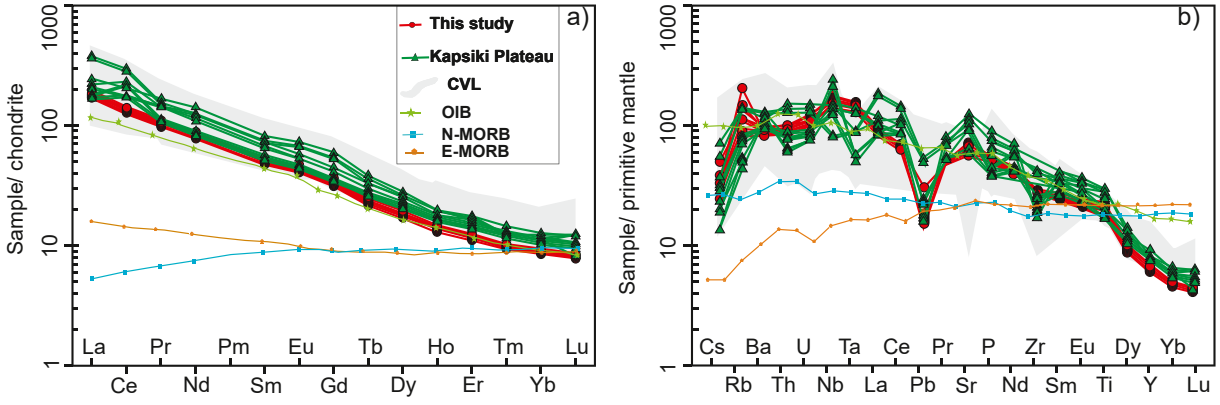

Fig. 7. a) Rare earth elements of the studied samples normalised to chondrite of Anders and Grevesse (1989); b) Concentrations of trace elements normalised to the primitive mantle and data for OIB, N-MORB, and E-MORB after Sun and McDonough (1989).

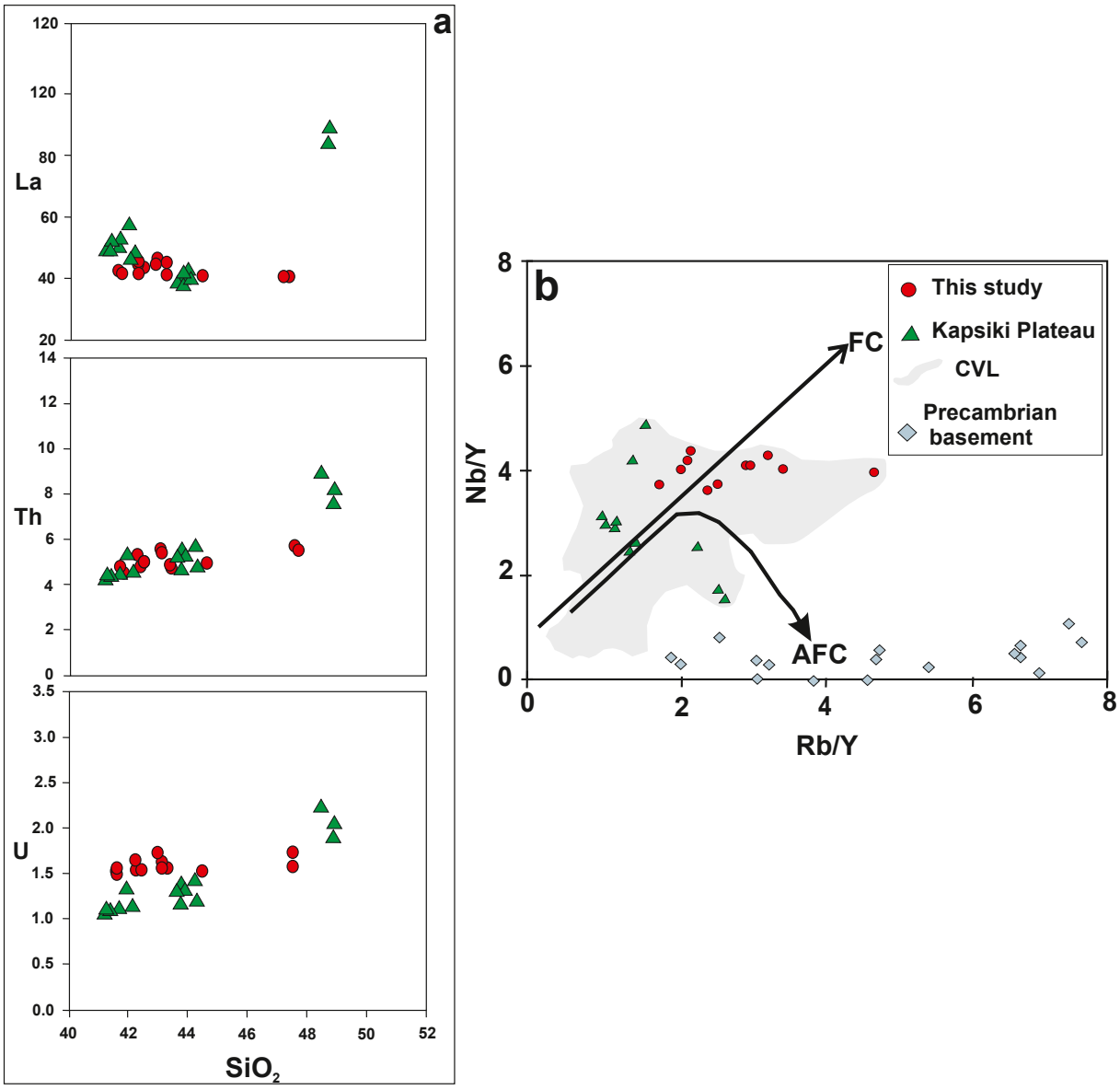

Fig. 8. a) Variations in LILE (ppm) for the studied lavas and other mafic lavas of the Kapsiki Plateau plotted against SiO_2 (wt.%); b) Nb/Y *vs.* Rb/Y diagram after Cox and Hawkesworth (1985) and Leeman and Hawkesworth (1986) showing basement samples relative to the lava compositions. Precambrian basement data are from Ganwa et al. (2011) and Tchameni et al. (2016).

ratio variations. The small negative Pb, Th, and Zr spikes in Fig. 7b support the existence of a metasomatic effect.

5.5. Implications for the formation of the CVL

The geochemical variations in the mafic Moukoulvi lavas contrast with those in other sectors of the CVL. The CVL magmatism is thought to be caused by a combination of factors, such as the metasomatism-related composition of the mantle source, potential participation of pyroxenite in the melting process, the depth of partial melting within the stability fields of spinel or garnet, and the characteristics and location of the mantle source (Nkouandou et al., 2008; Ngongang Tchikankou et al., 2020). This study includes details on possible crustal recycling and/or mantle metasomatism that may have influenced mantle heterogeneity in this area of the CVL, as well as other basaltic lavas of the Adamawa Plateau (Nkouandou et al., 2015; Njombie Wagsong et al., 2018, 2021; Temdjim et al., 2019). Numerous studies (Marzoli et al., 2000; Kamgang et al., 2013; Tchuimegnie Ngongang et al., 2015; Tiabou et al., 2019) suggest that the peridotite mantle is the principal source of melts associated with OIB. These melts are produced by the partial melting of peridotite under different pressure and temperature conditions. The multi-element normalised diagrams to Sun and McDonough (1989) of the Moukoulvi lavas (Fig. 7b) are comparable to those reported from other volcanoes along the CVL, with HREE depletion and LREE enrichment, indicating the presence and enrichment of garnet in the source. The CVL magmas traversed through a Precambrian basement and have probably undergone

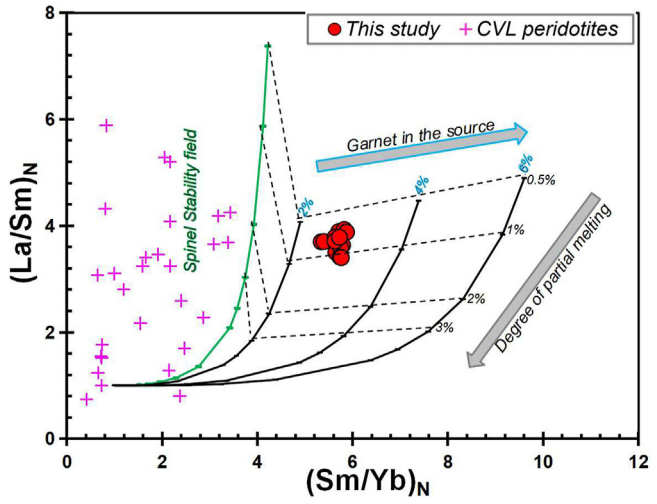

Fig. 9. Melting results for Moukoulvi lavas modelled on a plot of $(Sm/Yb)_N$ *vs.* $(La/Sm)_N$. Trace element data for peridotites are from Lee et al. (1996), Tamen et al. (2007), Sababa et al. (2015), Tedonkenfack et al. (2019), and Asaah (2015, 2021).

contamination, similar to other intraplate continental alkaline magmas. Therefore, the basement enclaves in the examined samples and the presence of assimilation fractional crystallisation provide evidence that the magmatism of the Moukoulvi lavas is connected to the continental crust. HFSE ratios (Zr/Hf, Nb/Ta, and U/Th) are similar, suggesting that the lavas came from a reasonably homogeneous mantle source. Several different mantle components may not be involved as much as these constant ratios indicate. This level of partial melting for Moukoulvi lavas is comparable to what is recorded in other CVL volcanoes (Asaah, 2015; Asaah et al., 2015a, 2015b; Gountié Dedzo et al., 2019; Kamgang et al., 2013; Yokoyama et al., 2007; Njombie Wagsong et al., 2021; Tchouhla et al., 2023). The consensus widely acknowledges that variations in trace element ratios and HFSE within CVL lavas can be elucidated by the influence of metasomatism on the source (Asaah et al., 2020). In contrast to the most recent lavas, older lavas from the CVL usually show less radiogenic Pb, suggesting non-uniform metasomatism throughout the line (Asaah et al., 2021). The volcanic activity of the Kapsiki Plateau has been estimated to be between 35 and 27 Ma (Vincent and Armstrong, 1973; Dunlop, 1983), suggesting that the melting source has not shifted in conjunction with the African plate. The absence of temperature anomalies in the upper mantle beneath the CVL has been repeatedly demonstrated by geophysical investigations (Reusch et al., 2010, 2011; Adams et al., 2015). This eliminates the possibility of a mantle plume in this region and reveals an anomalously convecting upper mantle material upwelling from the 660 km discontinuity, which may be a passive reaction to lithospheric disintegration (Courtillot et al., 2003). Thus, the magma erupted from the CVL as a result of the lithosphere breaking due to the hot mantle material upwelling.

6. Conclusions

The Moukoulvi lavas are primarily basalts and basanites, with an alkaline composition, similar to most of the mafic rocks in the northern part of the CVL. The petrographic investigation revealed a microlithic porphyritic texture mineral assemblage dominated by olivine and clinopyroxene phenocrysts, together with plagioclase microcrysts. The magmas experienced fractionation of the major phenocryst phases, olivine and clinopyroxene, which were accompanied by iron and titanium oxide, along with apatite. All the fractionated phases, except for the apatite, were identified as components in thin sections. The lack of correlations between Th, La, U, and SiO_2 indicates the absence of interaction with the continental crust, which is further supported by the trend of the samples plotted on the Nb/Y vs. Rb/Y diagram (Fig. 8). The occurrence of olivine and clinopyroxene phenocrysts also indicates that magma is ascending quickly, reducing the possibility of crustal contamination. The mantle source of the Moukoulvi lavas is inferred to be enriched, with evidence of partial melting occurring at depths corresponding to the stability field of garnet. The Moukoulvi lavas have traits in line with OIB patterns as well as evidence of metasomatism and mantle heterogeneity.

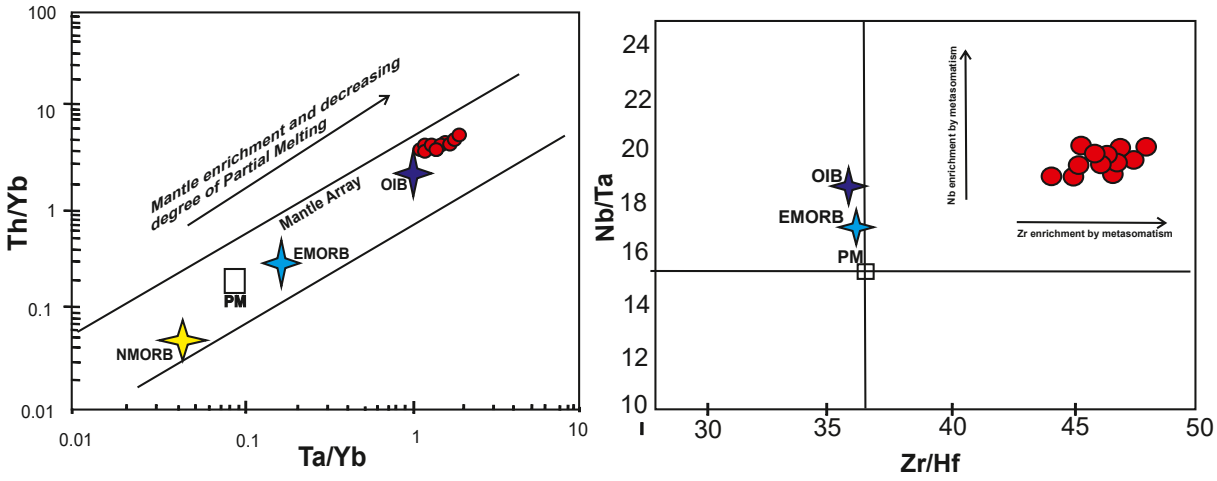

Fig. 10. a) Ta/Yb *vs.* Th/Yb diagram with the Moukoulvi lavas plotting on the typical OIB mantle array; b) Zr/Hf *vs.* Nb/Ta showing variable enrichment in HFSE.

According to the high values in LREE and relative enrichment in HFSE, the lavas, resembling most sodic alkaline continental magmas in the CVL, likely originate from a diverse mantle source. The lack of anomalies in temperature in the upper mantle under the CVL implies that the magmatism originates from the lithospheric mantle source instead of a mantle plume. The presence of a Pb depletion (Ce/Pb > 30) also implies that these magmas belong to the HIMU-OIB type, attributed to lithospheric mantle metasomatism.

CRediT authorship contribution statement

Diddi Hamadjoda Djamilatou: Writing – original draft, Visualization, Validation, Software, Resources, Methodology, Investigation, Funding acquisition, Formal analysis, Data curation, Conceptualization. **Merlin Gountié Dedzo:** Writing – original draft, Visualization, Validation, Supervision, Software, Resources, Project administration, Methodology, Investigation, Formal analysis, Data curation, Conceptualization. **Nils Lenhardt:** Writing – original draft, Visualization, Validation, Supervision, Software, Resources, Project administration, Methodology, Investigation, Formal analysis, Data curation, Conceptualization. **Désiré Tsozué:** Writing – original draft, Visualization, Validation, Supervision, Software, Resources, Project administration, Methodology, Investigation, Data curation. **Asobo Nkengmatia Elvis Asaah:** Writing – original draft, Visualization, Validation, Software, Resources, Methodology, Investigation, Formal analysis, Data curation. **Moussa Ngarena Klamadji:** Writing – original draft, Software, Resources, Methodology, Investigation, Data curation.

Source of support

Any grants/equipment/drugs, and/or other support that facilitated the conduct of research/writing of the manuscript (including AFMRC project details, if applicable): The Organization for Women in Science for the Developing World (OWSD) and the Swedish International Development Cooperation Agency (SIDA) “Grant No: 3241318611”.

Declaration of competing interest

The authors have no conflicts of interest to declare.

All co-authors have seen and agree with the contents of the manuscript and there is no financial interest to report. We certify that the submission is original work and is not under review at any other publication.

Acknowledgements

This work constitutes part of the first author's PhD thesis. It was carried out with the support of the fellowship “Organization for Women in Science for the Developing World (OWSD) and the Swedish International Development Cooperation Agency (SIDA)”. We thank the editor Weidong Sun and anonymous reviewers for proper handling and important observations made to improve the quality of this contribution. We are grateful to Erepamo Omietimi, Jeannette Dykstra, Wiebke Grote and Noxolo Noxy for their assistance during the laboratory work.

References

Adams, A.N., Wiens, D.A., Nyblade, A.A., Euler, G.G., Shore, P.J., Tibi, R., 2015. Lithospheric instability and the source of the Cameroon Volcanic Line: evidence from Rayleigh wave phase velocity tomography. J. Geophys. Res. Solid Earth 120, 1708–1727.

Adjia, H.Z., Villiéras, F., Kamga, R., Thomas, F., 2013. Mineralogy and physico-chemical properties of alluvial clays from far North region of Cameroon: a tool for an environmental problem. Int. J. Water Resour. Environ. Eng. 5, 54–66.

Albino, F., Biggs, J., 2021. Magmatic processes in the East African Rift system: insights from a 2015–2020 sentinel-1 InSAR survey. Geochem. Geophys. Geosystems 22, e2020GC009488.

Anders, E., Grevesse, N., 1989. Abundances of the elements: meteoritic and solar. Geochem. Cosmochim. Acta 53, 197–214.

Asaah, A.N., Yokoyama, T., Aka, F.T., Usui, T., Kuritani, T., Wirmvem, M.J., Iwamori, H., Fozing, E.M., Tamen, J., Mofor, G.Z., 2015a. Geochemistry of lavas from maar-bearing volcanoes in the Oku volcanic group of the Cameroon volcanic line. Chem. Geol. 406, 55–69.

Asaah, A.N., Yokoyama, T., Aka, F.T., Usui, T., Wirmvem, M.J., Tchamabe, B.C., Ohba, T., Tanyileke, G., Hell, J.V., 2015b. A comparative review of petrogenetic processes beneath the Cameroon Volcanic Line: geochemical constraints. Geosci. Front. 6, 557–570.

Asaah, A.N.E., Yokoyama, T., Aka, F.T., Iwamori, H., Kuritani, T., Usui, T., Dedzo, M.G., Tamen, J., Hasegawa, T., Fozing, E.M., 2020. Major/trace elements and Sr–Nd–Pb isotope systematics of lavas from lakes Barombi Mbo and Barombi Koto in the Kumba graben, Cameroon volcanic line: constraints on petrogenesis. J. Afr. Earth Sci. 161, 103675.

Asaah, A.N.E., Yokoyama, T., Iwamori, H., Aka, F.T., Kuritani, T., Usui, T., Tamen, J., Gountié Dedzo, M., Chako Tchamabé, B., Hasegawa, T., Nche, L.A., Ohba, T., 2021. High-μ signature in lavas of Mt. Oku: implications for lithospheric and asthenospheric contributions to the magmatism of the Cameroon Volcanic Line (West Africa). Lithos 400–401, 106416.

Barrat, J.A., Boulegue, J., Tiercelin, J.J., Lesourd, M., 2000. Strontium isotopes and rare-earth element geochemistry of hydrothermal carbonate deposits from Lake Tanganyika, East Africa. Geochem. Cosmochim. Acta 64, 287–298.

Biggs, J., Bastow, I.D., Keir, D., Lewi, E., 2011. Pulses of deformation reveal frequently recurring shallow magmatic activity beneath the Main Ethiopian Rift. Geochem. Geophys. Geosystems 12.

Bilong, P., Ndjigui, P.-D., Temdjim, R., Sababa, E., 2011. Geochemistry of peridotite and granite xenoliths during the early stage of weathering in the Nyos volcanic region (NW Cameroon): implications for PGE exploration. Geochemistry 71, 77–86.

Burke, K., 2001. Origin of the Cameroon line of volcano-capped swells. J. Geol. 109, 349–362.

Bute, S.I., Yang, X.-Y., Cao, J., Liu, L., Deng, J.-H., Haruna, I.V., Girei, M.B., Abubakar, U., Akhtar, S., 2019. Origin and tectonic implications of ferroan alkalicalcic granitoids from the Hawal Massif, east-eastern Nigeria terrane: clues from geochemistry and zircon U-Pb Hf isotopes. Int. Geol. Rev. 62, 129–152.

Cantagrel, R., Carles, J., 1978. Caractérisation analytique des vins de cépage et phénomènes de vieillissement. Annales de La Nutrition et de l'alimentation 1073–1094. JSTOR.

Chako Tchamabé, B., Ohba, T., Kereszturi, G., Németh, K., Aka, F.T., Youmen, D., Miyabuchi, Y., Ooki, S., Tanyileke, G., Hell, J.V., 2015. Towards the reconstruction of the shallow plumbing system of the Barombi Mbo Maar (Cameroon) implications for diatreme growth processes of a polygenetic maar volcano. J. Volcanol. Geoth. Res. 301, 293–313.

Chenyi, M.-L.V., Nkouathio, D.G., Wotchoko, P., Nono, G.D.K., Zenon, I., Guedjeo, C.S., Seuwui, D.T., 2017. Volcanology and geochemical study of the volcanic rocks of the Bafmeng area (Mount Oku, Cameroon volcanic line). Int. J. Biol. Chem. Sci. 11, 941–964.

Chorowicz, J., 2005. The east African rift system. J. Afr. Earth Sci. 43, 379–410.
Cornacchia, M., Dars, R., 1983. Un trait structural majeur du continent Africain; les lineaments centrafricains du Cameroun au Golfe d'Aden. Bull. Société Géologique Fr 7, 101–109.
Coulon, C., Vidal, P., Dupuy, C., Baudin, P., Popoff, M., Maluski, H., Hermitte, D., 1996. The Mesozoic to early Cenozoic magmatism of the Benue Trough (Nigeria); geochemical evidence for the involvement of the St Helena plume. J. Petrol. 37, 1341–1358.
Courtillot, V., Davaille, A., Besse, J., Stock, J., 2003. Three distinct types of hotspots in the Earth's mantle. Earth Planet Sci. Lett. 205, 295–308.
Cox, K.G., Hawkesworth, C.J., 1985. Geochemical stratigraphy of the Deccan Traps at Mahabaleshwar, Western Ghats, India, with implications for open system magmatic processes. J. Petrol. 26, 355–377.
Déruelle, B., Ngounouno, I., Demaiffe, D., 2007. The 'Cameroon Hot Line'(CHL): a unique example of active alkaline intraplate structure in both oceanic and continental lithospheres. Comptes Rendus Geosci 339, 589–600.
Dunlop, H.M., 1983. Strontium isotope geochemistry and potassium-argon studies on volcanic rocks from the Cameroon line, West Africa. PhD thesis, 347p. Univrsity of Edinburgh.
Dunlop, H.M., Fitter, J.G., 1979. A K-Ar and Sr-isotopic study of the volcanic rocks of the island of Principe, West Africa—evidence for mantle heterogeneity beneath the Gulf of Guinea. Contrib. Mineral. Petrol. 71, 125–131.
Fitton, J.G., 1980. The Benue trough and Cameroon line—a migrating rift system in West Africa. Earth Planet Sci. Lett. 51, 132–138.
Fitton, J.G., 1987. The Cameroon line, West Africa: a comparison between oceanic and continental alkaline volcanism. Geol. Soc. Lond. Spec. Publ. 30, 273–291.
Foley, S., 1992. Vein-plus-wall-rock melting mechanisms in the lithosphere and the origin of potassic alkaline magmas. Lithos 28, 435–453.
Frey, F.A., Green, D.H., Roy, S.D., 1978. Integrated models of basalt petrogenesis: a study of quartz tholeiites to olivine melilitites from south eastern Australia utilizing geochemical and experimental petrological data. J. Petrol. 19, 463–513.
Furman, T., 2007. Geochemistry of East African rift basalts: an overview. J. Afr. Earth Sci. 48, 147–160.
Ganwa, A.A., Siebel, W., Frisch, W., Shang, K.C., 2011. Geochemistry of magmatic rocks and time constraints on deformational phases and shear zone slip in the Méiganga area, central Cameroon. Int. Geol. Rev. 53, 759–784.
Ganwa, A.A., Klötzli, U.S., Hauzenberger, C., 2016. Evidence for Archean inheritance in the pre-Panafrican crust of Central Cameroon: insight from zircon internal structure and LA-MC-ICP-MS UPb ages. J. Afr. Earth Sci. 120, 12–22.
Geiger, H., Barker, A.K., Troll, V.R., 2016. Locating the depth of magma supply for volcanic eruptions, insights from Mt. Cameroon. Sci. Rep. 6, 33629.
Gouhier, J., Rollet, M., 1978. la structure annulaire de Golda-Zuelva (Cameroun). SOCIETE GEOL. FRANCE; DA. 1978, p. 189. BIBL. 1 REF.
Gountié Dedzo, M., Asaah, A.N.E., Fozing, E.M., Tchamabé, B.C., Zangmo, G.T., Dagwai, N., Seuwui, D.T., Kamgang, P., Aka, F.T., Ohba, T., 2019. Petrology and geochemistry of lavas from Gawar, Minawao and Zamay volcanoes of the northern segment of the Cameroon volcanic line (Central Africa): constraints on mantle source and geochemical evolution. J. Afr. Earth Sci. 153, 31–41.
Gountié Dedzo, M., Djamilatou, D.H., Fozing, E.M., Tchamabé, B.C., Mendoza-Rosas, A.T., Asaah, A.N.E., Tefogoum, G.Z., Kamgang, P., Ohba, T., 2020. Petrology and geochemistry of ignimbrites and associated enclaves from mount Bambouto, West-Cameroon, Cameroon volcanic line. Geochemistry 80, 125663.
Gountié Dedzo, M., Fozing, E.M., Chako-Tchamabé, B., Biakan à Nyotok, P.C., Djamilatou, D.H., Asaah, A.N.E., Zangmo Tefogoum, G., Kamgang, P., Ohba, T., 2022. Geochemical features and petrology of ignimbrite deposits from Bamenda volcano, Western Highlands of the Cameroon volcanic line. Arabian J. Geosci. 15, 643.
Grant, A.C., 1972. The continental margin off Labrador and eastern Newfoundland–morphology and geology. Can. J. Earth Sci. 9, 1394–1430.
Green, P.F., 1980. On the cause of the shortening of spontaneous fission tracks in certain minerals. Nucl. Tracks 4, 91–100.
Green, P.F., Duddy, I.R., Laslett, G.M., Hegarty, K.A., Gleadow, A.W., Lovering, J.F., 1989. Thermal annealing of fission tracks in apatite 4. Quantitative modelling techniques and extension to geological timescales. Chem. Geol. Isot. Geosci. Sect. 79, 155–182.
Guiraud, M., 1990. Tectono-sedimentary framework of the early Cretaceous continental Bima formation (upper Benue Trough, NE Nigeria). J. Afr. Earth Sci. 10, 341–353.
Halliday, A.N., Davidson, J.P., Holden, P., DeWolf, C., Lee, D.-C., Fitton, J.G., 1990. Trace-element fractionation in plumes and the origin of HIMU mantle beneath the Cameroon line. Nature 347, 523–528.
Halliday, A.N., Lee, D.-C., Tommasini, S., Davies, G.R., Paslick, C.R., Fitton, J.G., James, D.E., 1995. Incompatible trace elements in OIB and MORB and source enrichment in the sub-oceanic mantle. Earth Planet Sci. Lett. 133, 379–395.
Halliday, A.N., Lee, D.-C., Christensen, J.N., Rehkämper, M., Yi, W., Luo, X., Hall, C.M., Ballentine, C.J., Pettke, T., Stirling, C., 1998. Applications of multiple collector-ICPMS to cosmochemistry, geochemistry, and paleoceanography. Geochem. Cosmochim. Acta 62, 919–940.
Hofmann, A.W., 2003. Sampling mantle heterogeneity through oceanic basalts: isotopes and trace elements. Treatise Geochem. 2, 568.
Hofmann, A.W., Jochum, K.P., Seufert, M., White, W.M., 1986. Nb and Pb in oceanic basalts: new constraints on mantle evolution. Earth Planet Sci. Lett. 79, 33–45.
Hutchison, W., Biggs, J., Mather, T.A., Pyle, D.M., Lewi, E., Yirgu, G., Caliro, S., Chiodini, G., Clor, L.E., Fischer, T.P., 2016. Causes of unrest at silicic calderas in the East African Rift: new constraints from InSAR and soil-gas chemistry at Aluto volcano, Ethiopia. Geochem. Geophys. Geosystems 17, 3008–3030.
Irvine, T.N., Baragar, W.R.A., 1971. A guide to the chemical classification of the common volcanic rocks. Can. J. Earth Sci. 8, 523–548.
Jung, S., Masberg, P., 1998. Major-and trace-element systematics and isotope geochemistry of Cenozoic mafic volcanic rocks from the Vogelsberg (central Germany): constraints on the origin of continental alkaline and tholeiitic basalts and their mantle sources. J. Volcanol. Geoth. Res. 86, 151–177.
Kagou, Dongmo A., Nkouathio, D., Pouclet, A., Bardintzeff, J.-M., Wandji, P., Nono, A., Guillou, H., 2010. The discovery of late Quaternary basalt on Mount Bambouto: implications for recent widespread volcanic activity in the southern Cameroon Line. J. Afr. Earth Sci. 57, 96–108.
Kamgang, P., Chazot, G., Njonfang, E., Ngongang, N.B.T., Tchoua, F.M., 2013. Mantle sources and magma evolution beneath the Cameroon Volcanic Line: geochemistry of mafic rocks from the Bamenda Mountains (NW Cameroon). Gondwana Res. 24, 727–741.
Kamguia, J., Nouayou, R., Tabod, C.T., Tadjou, J.M., Manguelle-Dicoum, E., Kande, H.L., 2008. Geophysical signature of geological units inferred from the analysis of geoid maps in Cameroon and its surroundings. J. Afr. Earth Sci. 52, 1–8.
Konfor, N., Temdjim, R., Richard, C., Ghogomub, N., Tchuitchoub, R., Ajoninac, H., 2007. Geochemistry of tertiary-quaternary lavas of Mt. Oku Northwest Cameroon. Rev. Fac. Ing. Univ. Antioquia 59–75.
Lapi, P.N., Amobi, J.O., Ofoma, A.E., Ezepue, M.C., 2006. Comparative geochemical study of the 1982 and 1999 Mount Cameroon volcanic eruptions, South-West Province, Cameroon. Global J. Pure Appl. Sci. 12, 559–572.
Le Bas, M., Le Maitre, R., Streckeisen, A., Zanettin, B., 1986. A chemical classification of volcanic rocks based on the total alkali-silica diagram. J. Petrol. 27, 745–750.
Lee, D.C., Halliday, A.N., Davies, G.R., Essene, E.J., Fitton, J.G., Temdjim, R., 1996. Melt enrichment of shallow depleted mantle: a detailed petrological, trace element and isotopic study of mantle–derived xenoliths and megacrysts from the Cameroon Line. J. Petrol. 37, 415–441.
Leeman, W.P., Hawkesworth, C.J., 1986. Open magma systems: trace element and isotopic constraints. J. Geophys. Res. Solid Earth 91, 5901–5912.
Lenhardt, N., Oppenheimer, C., 2014. Volcanism in Africa: geological perspectives, hazard assessment and societal implications. In: Ismail-Zadeh, A., Urrutia-Fucugauchi, J., Kijko, A., Takeuchi, K., Zaliapin, I.

(Eds.), Extreme Natural Hazards, Disaster Risks and Societal Implications, IUGG Special Publication Series, vol. 1. Cambridge University Press, pp. 169–199.
Loubser, M., Verryn, S., 2008. Combining XRF and XRD analyses and sample preparation to solve mineralogical problems. S. Afr. J. Geol. 111, 229–238.
Marzoli, A., Renne, P.R., Piccirillo, E.M., Francesca, C., Bellieni, G., Melfi, A.J., Nyobe, J.B., N'ni, J., 1999. Silicic magmas from the continental Cameroon Volcanic Line (Oku, Bambouto and Ngaoundere): 40 Ar-39 Ar dates, petrology, Sr-Nd-O isotopes and their petrogenetic significance. Contrib. Mineral. Petrol. 135, 133–150.
Marzoli, A., Piccirillo, E.M., Renne, P.R., Bellieni, G., Iacumin, M., Nyobe, J.B., Tongwa, A.T., 2000. The Cameroon Volcanic Line revisited: petrogenesis of continental basaltic magmas from lithospheric and asthenospheric mantle sources. J. Petrol. 41, 87–109.
Marzoli, A., Aka, F.T., Merle, R., Callegaro, S., N'ni, J., 2015. Deep to shallow crustal differentiation of within-plate alkaline magmatism at Mt. Bambouto volcano, Cameroon Line. Lithos 220, 272–288.
Mebara Onana, F.X.,M., Temdjim, R., Njombie Wagsong, M.P., Chazot, G., Feudjio Tiabou, A., Mouafo, L., Njonfang, E., 2022. Petrography, mineral chemistry and geochemistry of quaternary volcanism from Wakwa plain, Adamawa massif (Cameroon volcanic line, West-central Africa). Arabian J. Geosci. 15, 1106.
Merle, R., Marzoli, A., Aka, F.T., Chiaradia, J.M., Reisberg, L., Castorina, F., Jourdan, F., Renne, P.R., N'ni, J., Nyobe, J.B., 2017. Mt Bambouto Volcano, Cameroon Line: mantle source and differentiation of within-plate alkaline rocks. J. Petrol. 58, 933–962.
Middlemost, E.A., 1975. The basalt clan. Earth Sci. Rev. 11, 337–364.
Moreau, M., 1987. L'approche structurelle en travail social: implications pratiques d'une approche intégrée conflictuelle. Serv. Soc. 36, 227–247.
Moundi, A., Wandji, P., Bardintzeff, J.-M., Ménard, J.-J., Atouba, L.C.O., Mouncherou, O.F., Reusser, É., Bellon, H., Tchoua, F.M., 2007. Les basaltes éocènes à affinité transitionnelle du plateau Bamoun, témoins d'un réservoir mantellique enrichi sous la ligne volcanique du Cameroun. Comptes Rendus Geosci 339, 396–406.
Nemzoue, P.N.N., Keutchafo, N.A.K., Tchouankoue, J.P., 2020. Geothermal development in Cameroon. Rev. Eng. Térmica 19, 32–41.
Nformidah-Ndah, S.S., Tollan, P.M., Hermann, J., Tchouankoue, J.P., 2022. Depletion and refertilisation of the lithospheric mantle below the Kapsiki plateau (Northern Cameroon Volcanic Line) deduced from trace element and H2O systematics in mantle xenoliths. J. Afr. Earth Sci. 189, 104483.
Ngongang Tchikankou, L.N., Kamgang, P., Chazot, G., Agranier, A., Bellon, H., Nonnotte, P., Ngongang, N.B.T., Kwekam, M., 2020. Mantle source evolution beneath the Cameroon volcanic line: geochemical and geochronological evidence from Fotouni volcanic series, Western Cameroon. Arabian J. Geosci. 13, 1–20.
Ngounouno, I., 1993. Pétrologie du magmatisme cénozoïque de la vallée de la Bénoué et du plateau Kapsiki (nord du Cameroun). PhD Thesis, Pierre et Marie Curie University, Paris, 280 pp.
Ngounouno, I., Déruelle, B., Demaiffe, D., 2000. Petrology of the bimodal Cenozoic volcanism of the Kapsiki Plateau (northernmost Cameroon, central Africa). J. Volcanol. Geoth. Res. 102, 21–44.
Ngwa, C.N., Lenhardt, N., Le Roux, P., Mbassa, B.J., 2019. The Mount Cameroon southwest flank eruptions: geochemical constraints on the subsurface magma plumbing system. J. Volcanol. Geoth. Res. 384, 179–188.
Ngwa, C.N., Shu, B.N., Mbassa, B.J., 2021. Clinopyroxene and olivine-hosted spinel inclusions from the Mt Cameroon volcanic area, west-central Africa. J. Afr. Earth Sci. 181, 104245.
Nicholson, H., Condomines, M., Fitton, J.G., Fallick, A.E., Grönvold, K., Rogers, G., 1991. Geochemical and isotopic evidence for crustal assimilation beneath Krafla, Iceland. J. Petrol. 32, 1005–1020.
Njombie Wagsong, P.M., Temdjim, R., Foley, S.F., 2018. Petrology of spinel lherzolite xenoliths from Youkou volcano, Adamawa Massif, Cameroon Volcanic Line: mineralogical and geochemical fingerprints of sub-rift mantle processes. Contrib. Mineral. Petrol. 173 (13), 1–20.
Njombie Wagsong, P.M., Temdjim, R., Tchuimegnie, N.B.N., Foley, S.F., Mebara, F.X.O., 2021. Pyroxenite in the mantle source of basanites at the Youkou Maar, Adamawa volcanic massif (Cameroon volcanic line, West Africa). Chem. Geol. 583, 120478.
Njome, M.S., de Wit, M.J., 2014. The Cameroon Line: analysis of an intraplate magmatic province transecting both oceanic and continental lithospheres: constraints, controversies and models. Earth Sci. Rev. 139, 168–194.
Njome, M.S., Suh, C.E., Sparks, R.S.J., Ayonghe, S.N., Fitton, J.G., 2008. The Mount Cameroon 1959 compound lava flow field: morphology, petrography and geochemistry. Swiss J. Geosci. 101, 85–98.
Njonfang, E., Nono, A., Kamgang, P., Ngako, V., Tchoua, F.M., 2011. Cameroon Line alkaline magmatism (central Africa): a reappraisal. Geol. Soc. Am. Spec. Pap. 478, 173–192.
Nkouandou, O.F., Temdjim, R., 2011. Petrology of spinel lherzolite xenoliths and host basaltic lava from Ngao Voglar volcano, Adamawa Massif (Cameroon Volcanic Line, West Africa): equilibrium conditions and mantle characteristics. J. Geosci. 56, 375–387.
Nkouandou, O.F., Ngounouno, I., Déruelle, B., Ohnenstetter, D., Montigny, R., Demaiffe, D., 2008. Petrology of the mio-pliocene volcanism to the north and east of Ngaoundéré (Adamawa, Cameroon). Comptes Rendus Geosci 340, 28–37.
Nkouandou, O.F., Bardintzeff, J.-M., Fagny, A.M., 2015. Sub-continental lithospheric mantle structure beneath the Adamawa plateau inferred from the petrology of ultramafic xenoliths from Ngaoundéré (Adamawa plateau, Cameroon, Central Africa). J. Afr. Earth Sci. 111, 26–40.
Nkouathio, D.G., Kagou Dongmo, A., Bardintzeff, J.M., Wandji, P., Bellon, H., Pouclet, A., 2008. Evolution of volcanism in graben and horst structures along the Cenozoic Cameroon Line (Africa): implications for tectonic evolution and mantle source composition. Mineral. Petrol. 94, 287–303.
Okomo Atouba, L.C., Chazot, G., Moundi, A., Agranier, A., Bellon, H., Nonnotte, P., Nzenti, J.-P., Kankeu, B., 2016. Mantle sources beneath the Cameroon Volcanic Line: geochemistry and geochronology of the Bamoun plateau mafic rocks. Arabian J. Geosci. 9, 1–12.
Poudjom Djomani, Y., Nnange, J.M., Diament, M., Ebinger, C.J., Fairhead, J.D., 1995. Effective elastic thickness and crustal thickness variations in west central Africa inferred from gravity data. J. Geophys. Res. Solid Earth 100, 22047–22070.
Rankenburg, K., Lassiter, J.C., Brey, G., 2004. Origin of megacrysts in volcanic rocks of the Cameroon volcanic chain–constraints on magma genesis and crustal contamination. Contrib. Mineral. Petrol. 147, 129–144.
Rankenburg, K., Lassiter, J.C., Brey, G., 2005. The role of continental crust and lithospheric mantle in the genesis of Cameroon volcanic line lavas: constraints from isotopic variations in lavas and megacrysts from the Biu and Jos Plateaux. J. Petrol. 46, 169–190.
Regnoult, J.-M., 1986. Synthèse géologique du Cameroun. Ministère des mines et de l'energie.
Reusch, A.M., Nyblade, A.A., Wiens, D.A., Shore, P.J., Ateba, B., Tabod, C.T., Nnange, J.M., 2010. Upper mantle structure beneath Cameroon from body wave tomography and the origin of the Cameroon Volcanic Line. Geochem. Geophys. Geosystems 11.
Reusch, A.M., Nyblade, A.A., Tibi, R., Wiens, D.A., Shore, P.J., Bekoa, A., Tabod, C.T., Nnange, J.M., 2011. Mantle transition zone thickness beneath Cameroon: evidence for an upper mantle origin for the Cameroon Volcanic Line. Geophys. J. Int. 187, 1146–1150.
Rolet, J., Mondeguer, A., Bouroullec, J.-L., Bandora, T., Coussement, C., Rehault, J.-P., Tiercelin, J.-J., 1991. Structure and different kinematic development faults along the lake Tanganyika rift-valley (East-African Rift System). Bull. Cent. Rech. Explor.-Prod. Elf-Aquitaine 15, 327–342.
Rollinson, Hugh R., 1993. Using geochemical data. evaluation. Present. Interpret. 796, 317.
Rooney, T.O., 2017. The Cenozoic magmatism of East-Africa: Part I—Flood basalts and pulsed magmatism. Lithos 286, 264–301.
Rooney, T.O., 2020. The cenozoic magmatism of east Africa: part V–magma sources and processes in the East African rift. Lithos 360, 105296.
Rooney, A.D., Macdonald, F.A., Strauss, J.V., Dudás, F.Ö., Hallmann, C., Selby, D., 2014. Re-Os geochronology and coupled Os-Sr isotope constraints on the Sturtian snowball Earth. Proc. Natl. Acad. Sci. USA 111, 51–56.

Saadat, S., Karimpour, M.H., Stern, C., 2010. Petrochemical characteristics of Neogene and quaternary alkali olivine basalts from the western margin of the Lut block, Eastern Iran.

Sababa, E., Ndjigui, P.D., Abeng, S.A.E., Bilong, P., 2015. Geochemistry of peridotite xenoliths from the Kumba and Nyos areas (southern part of the Cameroon Volcanic Line): implications for Au–PGE exploration. J. Geochem. Explor. 152, 75–90.

Sababa, E., Gentry, F.C., Ndjigui, P.-D., Onana, P.N., Seyoa, D.T., 2021. Petrography and geochemistry of sulfurous volcanic scoria from mount Cameroon area, Central Africa: implications for Au-PGE exploration. J. Afr. Earth Sci. 176, 104144.

Sato, H., Aramaki, S., Kusakabe, M., Hirabayashi, J., Sano, Y., Nojiri, Y., Tchoua, F., 1990. Geochemical difference of basalts between polygenetic and monogenetic volcanoes in the central part of the Cameroon volcanic line. Geochem. J. 24, 357–370.

Sebai, A., Feraud, G., Bertrand, H., Hanes, J., 1991. 40Ar/39Ar dating and geochemistry of tholeiitic magmatism related to the early opening of the Central Atlantic rift. Earth Planet Sci. Lett. 104, 455–472.

Sibuet, J.-C., Mascle, J., 1978. Plate kinematic implications of Atlantic equatorial fracture zone trends. J. Geophys. Res. Solid Earth 83, 3401–3421.

Suh, C.E., Ayonghe, S.N., Sparks, R.S.J., Annen, C., Fitton, J.G., Nana, R., Luckman, A., 2003. The 1999 and 2000 eruptions of Mount Cameroon: eruption behaviour and petrochemistry of lava. Bull. Volcanol. 65, 267–281.

Sun, S.-S., McDonough, W.F., 1989. Chemical and isotopic systematics of oceanic basalts: implications for mantle composition and processes. Geol. Soc. Lond. Spec. Publ. 42, 313–345.

Tamen, J., Nkoumbou, C., Mouafo, L., Reusser, E., Tchoua, F.M., 2007. Petrology and geochemistry of monogenetic volcanoes of the Barombi Koto volcanic field (Kumba graben, Cameroon volcanic line): implications for mantle source characteristics. C. R. Geosci. 339, 799–809.

Tamen, J., Nkoumbou, C., Reusser, E., Tchoua, F., 2015. Petrology and geochemistry of mantle xenoliths from the Kapsiki Plateau (Cameroon volcanic line): implications for lithospheric upwelling. J. Afr. Earth Sci. 101, 119–134.

Tchameni, R., Sun, F., Dawaï, D., Danra, G., Tékoum, L., Nomo Negue, E., Vanderhaeghe, O., Nzolang, C., Dagwaï, Nguihdama, 2016. Zircon dating and mineralogy of the Mokong Pan-African magmatic epidote-bearing granite (North Cameroon). Int. J. Earth Sci. 105, 1811–1830.

Tchop, L.J., Nguet, P.W., Ntieche, B., Metang, V., Rake, J.D., Teitchou, M.I., Vander Auwera, J., Ekodeck, G.E., Nkoumbou, C., 2020. New data on the genesis and evolution of the primitive magmas of Mount Cameroon: contribution of melt inclusions. J. Geol. Res. 2, 46–61.

Tchoua, M.F., 1974. Contribution a l'etude geologique et petrologique de quelques volcans de la ligne du Cameroun (Mont Manengouba et Bamboutos). These Doct Etat Univ Clermont Ferrand.

Tchouankoue, J.P., Wambo, N.A.S., Dongmo, A.K., Wörner, G., 2012. Petrology, geochemistry, and geodynamic implications of basaltic dyke swarms from the Southern Continental part of the Cameroon Volcanic Line, Central Africa.

Tchouhla, R., Dedzo, M.G., Chako-Tchamabé, B., Onana, G., Hamadjoda, D.D., Biakan à Nyotok, P.C., Ngarena, K.M., Asaah, A.N.E., Kamgang, P., 2023. Petrogenesis of lavas from Mokolo-Kosséhone region, northernmost segment of the Cameroon Volcanic Line: constraints from major/trace elements and Sr-Nd-Pb isotopic data. Geosci. J. 27, 139–160.

Tchuimegnie Ngongang, N.B., Kamgang, P., Chazot, G., Agranier, A., Bellon, H., Nonnotte, P., 2015. Age, geochemical characteristics and petrogenesis of Cenozoic intraplate alkaline volcanic rocks in the Bafang region, West Cameroon. J. Afr. Earth Sci. 102, 218–232.

Tedonkenfack, S.S.T., Tamen, J., Nkouathio, D.G., Asaah, A.N.E., Gountïe, M.D., Aka, F.T., 2019. Petrography and geochemistry of mantle xenoliths from the Ibal-Oku region (North-West region, Cameroon): preliminary evidence of mantle heterogeneities. J. Afr. Earth Sci. 154 (2019), 70–79.

Temdjim, R., Boivin, P., Chazot, G., Robin, C., Rouleau, É., 2004. L'hétérogénéité du manteau supérieur à l'aplomb du volcan de Nyos (Cameroun) révélée par les enclaves ultrabasiques. Comptes Rendus Geosci 336, 1239–1244.

Temdjim, R., Njombie Wagsong, P.M., Nzakou, T.J.A., Foley, S.F., 2019. Variation in mantle lithology and composition beneath the Ngao Bilta volcano, AdamawaMassif, Cameroon volcanic line, West-central Africa. Geosci. Front. 11, 665–677.

Tiabou, A.F., Temdjim, R., Wandji, P., Bardintzeff, J.-M., Che, V.B., Bate Tibang, E.E., Ngwa, C.N., Mebara, F.X.O., 2019. Baossi–Warack monogenetic volcanoes, Adamawa Plateau, Cameroon: petrography, mineralogy and geochemistry. Acta Geochim 38, 40–67.

Tokam, A.-P.K., Tabod, C.T., Nyblade, A.A., Julia, J., Wiens, D.A., Pasyanos, M.E., 2010. Structure of the crust beneath Cameroon, West Africa, from the joint inversion of Rayleigh wave group velocities and receiver functions. Geophys. J. Int. 183, 1061–1076.

Toteu, S.F., Michard, A., Bertrand, J.M., Rocci, G., 1987. U/Pb dating of Precambrian rocks from Northern Cameroon, orogenic evolution and chronology of the Pan-African belt of Central Africa. Precambr. Res. 37, 71–87.

Toteu, S.F., Van Schmus, W.R., Penaye, J., Michard, A., 2001. New U–Pb and Sm–Nd data from north-central Cameroon and its bearing on the pre-Pan African history of central Africa. Precambr. Res. 108, 45–73.

Tsafack, J.-P.F., Wandji, P., Bardintzeff, J.-M., Bellon, H., Guillou, H., 2009. The Mount Cameroon stratovolcano (Cameroon volcanic line, Central Africa): petrology, geochemistry, isotope and age data. Geochem. Mineral. Petrol. 47, 65–78.

Tsozué, D., Nzeugang, A.N., Mache, J.R., Loweh, S., Fagel, N., 2017. Mineralogical, physico-chemical, and technological characterization of clays from Maroua (Far-North, Cameroon) for use in ceramic bricks production. J. Build. Eng. 11, 17–24.

Ubangoh, R.U., Pacca, I.G., Nyobe, J.B., 1998. Palaeomagnetism of the continental sector of the Cameroon volcanic line, West Africa. Geophys. J. Int. 135, 362–374.

Vincent, P.M., Armstrong, R.L., 1973. Volcanism of the plateau Kapsiki (North Cameroon) and the underlying sedimentary formations. 7th Colloquim Afr. Geol. Florence Unpubl. Abstr. 1–12.

Vonopartis, L., Nex, P., Kinnaird, J., Robb, L., 2020. Evaluating the changes from endogranitic magmatic to magmatic-hydrothermal mineralization: the Zaaiplaats Tin Granites, Bushveld Igneous complex, South Africa. Minerals 10 (4), 379.

Wandji, P., Tsafack, J.P.F., Bardintzeff, J.M., Nkouathio, D.G., Kagou Dongmo, A., Bellon, H., Guillou, H., 2009. Xenoliths of dunites, wehrlites and clinopyroxenites in the basanites from Batoke volcanic cone (Mount Cameroon, Central Africa): petrogenetic implications. Mineral. Petrol. 96, 81–98.

Wheeler, W.H., Karson, J.A., 1994. Extension and subsidence adjacent to a "weak" continental transform: an example from the Rukwa rift, East Africa. Geology 22, 625–628.

Willbold, M., Stracke, A., 2006. Trace element composition of mantle endmembers: implications for recycling of oceanic and upper and lower continental crust. Geochem. Geophys. Geosystems 7.

Wilson, M., 1992. Magmatism and continental rifting during the opening of the South Atlantic Ocean: a consequence of Lower Cretaceous super-plume activity?. In: Storey, B.C., Alabaster, T., Pankhurst, R.J. (Eds.), Magmatism and the Causes of Continental Break-Up, vol. 68. Geological Society of London Special Publication, pp. 241–255.

Yamgouot, F.N., Déruelle, B., Mbowou, I.B.G., Ngounouno, I., Demaiffe, D., 2016. Geochemistry of the volcanic rocks from Bioko island ("Cameroon hot line"): evidence for plume-lithosphere interaction. Geosci. Front. 7, 743–757.

Yamgouot, F.N., Mbowou, I.B.G., Ngounouno, I., Abdoul, A., 2018. Insight into geochemistry of basaltic rocks from Mt Cameroon and characterization of the mantle source.

Yokoyama, T., Aka, F.T., Kusakabe, M., Nakamura, E., 2007. Plume–lithosphere interaction beneath Mt. Cameroon volcano, West Africa: constraints from 238U–230Th–226Ra and Sr–Nd–Pb isotope systematics. Geochem. Cosmochim. Acta 71, 1835–1854.

Ziegler, P.A., Cloetingh, S., 2004. Dynamic processes controlling evolution of rifted basins. Earth Sci. Rev. 64, 1–50.

Ziem à Bidias, L.A., Chazot, G., Moundi, A., Nonnotte, P., 2018. Extreme source heterogeneity and complex contamination patterns along the Cameroon Volcanic Line: new geochemical data from the Bamoun plateau. Comptes Rendus Geosci 350, 100–109.